

TRPM7-mediated spontaneous  $\text{Ca}^{2+}$  entry regulates the proliferation and differentiation of human  
leukaemia cell line K562

Kiriko Takahashi<sup>1,2\*</sup>, Chisato Umebayashi<sup>1,\*</sup>, Tomohiro Numata<sup>1,#</sup>, Akira Honda<sup>1</sup>, Jun Ichikawa<sup>1</sup>,  
Yaopeng Hu<sup>1</sup>, Ken Yamaura<sup>2</sup> and Ryuji Inoue<sup>1,#</sup>

<sup>1</sup>Department of Physiology, Fukuoka University School of Medicine

<sup>2</sup>Department of Anesthesiology, Fukuoka University School of Medicine.

\*contributed equally to this work.

#Authors for correspondence:

Ryuji Inoue, M.D., PhD.

Department of Physiology

Fukuoka University School of Medicine

[inouery@fukuoka-u.ac.jp](mailto:inouery@fukuoka-u.ac.jp)

Tomohiro Numata, PhD.

Department of Physiology

Fukuoka University School of Medicine

[numata@fukuoka-u.ac.jp](mailto:numata@fukuoka-u.ac.jp)

**Author contributions:**

K.T., mainly performed  $\text{Ca}^{2+}$  imaging, C.U. performed PCR, Western blotting and immunocytochemical experiments as well as  $\text{Ca}^{2+}$  imaging, functional assays, and T.N performed PCR, Western blotting as well as functional assays. A.H., J.I. and T.N. guided and assisted K.T. and C.U.; R.I. and Y. H. performed patch clamp experiments; K.Y. advised about the design of this study and gave comments during the course of the study; R.I., and T.N. conceived and designed the study and K.T., T.N. and R.I. wrote the paper.

Short title: TRPM7 mediates erythropoiesis in K562.

Key words: erythromyeloid cells, ERK-signalling, haemoglobin synthesis, spontaneous  $\text{Ca}^{2+}$  influx.

## Abstract

**AIM:** Continuous  $\text{Ca}^{2+}$  influx is essential to maintain intracellular  $\text{Ca}^{2+}$  homeostasis and its dysregulation leads to a variety of cellular dysfunctions. In this study, we explored the functional roles of spontaneous  $\text{Ca}^{2+}$  influx for the proliferation and differentiation of a human erythromyeloid leukaemia cell line K562.

**METHODS:** mRNA/protein expressions were assessed by the real-time RT-PCR, Western blotting and immunocytochemical staining. Intracellular  $\text{Ca}^{2+}$  concentration ( $[\text{Ca}^{2+}]_i$ ) and ionic currents were measured by fluorescent imaging and patch clamping techniques, respectively. Cell counting/viability and colorimetric assays were applied to assess proliferation rate and haemoglobin synthesis, respectively.

**RESULTS:** Elimination of extracellular  $\text{Ca}^{2+}$  decreased basal  $[\text{Ca}^{2+}]_i$  in proliferating K562 cells. Cation channel blockers such as SK&F96365, 2-APB,  $\text{Gd}^{3+}$  and FTY720 dose-dependently decreased basal  $[\text{Ca}^{2+}]_i$ . A spontaneously active inward current ( $I_{\text{spont}}$ ) contributive to basal  $[\text{Ca}^{2+}]_i$  was identified by the nystatin-perforated whole-cell recording.  $I_{\text{spont}}$  permeated  $\text{Ca}^{2+}$  comparably to  $\text{Na}^+$ , and was greatly eliminated by siRNA targeting TRPM7, a melastatin member of the transient receptor potential (TRP) superfamily. Consistent with these findings, TRPM7 immune-reactivity was detected by Western blotting, and immunofluorescence representing TRPM7 was found localized to the K562 cell membrane. Strikingly, all these procedures, i.e.  $\text{Ca}^{2+}$  removal, TRPM7 blockers and siRNA-mediated TRPM7 knockdown significantly retarded the growth and suppressed hemin-induced  $\gamma$ -

globin and haemoglobin syntheses in K562 cells, respectively, both of which appeared associated with the inhibition of ERK activation.

**CONCLUSIONS:** These results collectively suggest that spontaneous  $\text{Ca}^{2+}$  influx through constitutively active TRPM7 channels may critically regulate both proliferative and erythroid differentiation potentials of K562 cells.

(247 words)

#### Short Synopsis

The functional significance of spontaneous  $\text{Ca}^{2+}$  influx through TRPM7 channels in a human erythromyeloid leukaemia cell line K562 was investigated by  $\text{Ca}^{2+}$  imaging, patch clamping and biochemical assays with pharmacological and molecular biological interventions. The results suggest that the  $\text{Ca}^{2+}$  influx is crucial for the proliferation and erythroid differentiation of K562 cells, and point to the possibility that any defective gating of TRPM7 channel due to hereditary and/or acquired causes might lead to human hematopoietic disorders such as anaemia and thrombocytopenia.

## Introduction

$\text{Ca}^{2+}$  is a highly versatile intracellular signal that can regulate both acute and long-term cellular functions ranging from membrane excitation, contraction, neurotransmitter release, secretion, cell growth, differentiation to death<sup>1</sup>. In proliferating cells, for instance, a certain level of intracellular  $\text{Ca}^{2+}$  concentration ( $[\text{Ca}^{2+}]_i$ ) is crucial for the transcriptional/translational processes of cell cycle such as DNA replication and mitosis<sup>2-4</sup>. Thus, disruption of  $\text{Ca}^{2+}$  homeostasis and dynamics can lead to a variety of cellular pathophysiology in which numerous  $\text{Ca}^{2+}$ -mobilizing molecules including voltage-dependent Ca channels,  $\text{P}_{2\text{X}}$  and NMDA inotropic cation channels, Orai and TRP channels play pivotal roles (e.g.<sup>5,6</sup>).

TRPM7 is a melastatin subfamily member of transient receptor potential (TRP) protein, and has a unique structure dubbed the 'chanzyme' which contains both channel and kinase-like domains<sup>7,8</sup>. TRPM7 channel serves as a constitutively active transmembrane permeant pathway for  $\text{Ca}^{2+}$  and  $\text{Mg}^{2+}$ , as well as several essential and toxic trace metals<sup>9</sup>. The activity of TRPM7 is effectively regulated by intracellular  $\text{Mg}^{2+}$  and  $\text{MgATP}$  levels<sup>10</sup> and modified by phospholipase C-coupled signalling, endogenous  $\text{PIP}_2$  levels, growth factors, mechanical stress, reactive oxygen species, and extracellular acidity<sup>8,11,12</sup>. TRPM7 is expressed in almost all types of cells, and numerous studies have implicated this channel in cell fate-determining events such as survival, growth, differentiation and death<sup>8,10,13</sup>. Other lines of evidence also suggest close association of TRPM7 with embryonic development, cell morphogenesis/kinesis, inflammatory responses and tissue remodeling<sup>14-17</sup>.

K562 cells were established from a patient with chronic myeloid leukaemia and have extensively been used as suitable models to study not only leukaemogenesis but also abnormal haematopoiesis/differentiation into erythrocytic, megakaryocytic and monocytic lineages<sup>18</sup>. Stimulation by hemin (ferriprotoporphyrin IX), sodium butyrate or anthracyclines was shown to differentiate K562 cells to acquire the synthesizing capability of fetal-form haemoglobin (some part is  $\text{Ca}^{2+}$ -dependent), which thus provides a useful model representing erythropoiesis<sup>18-20</sup>.

In the present study, we sought the possible role for transmembrane  $\text{Ca}^{2+}$  influx in regulating proliferation and differentiation of K562 cells, with particular interest in TRPM7. This was prompted because the involvement of  $\text{Ca}^{2+}$  influx associated with endogenous TRP-like channels in K562 cells has been suggested for irradiation-induced cell cycle arrest and consequent survival of K562 cells<sup>21</sup>. In another study, a  $\text{Mg}^{2+}$ -dependent cation channel whose properties however differ from those of heterologously expressed TRPM7 has been identified in proliferating K562<sup>22</sup>. Moreover, we previously found that the critical contribution of TRPM7-mediated  $\text{Ca}^{2+}$  influx to the cell cycle transition at the G1/S boundary in human retinoblastoma cell<sup>23</sup>. To facilitate the stable recording of spontaneously active endogenous  $\text{Ca}^{2+}$  current as well as to better compare with the results obtained by different functional assays, we employed the nystatin-perforated whole-cell recording<sup>24</sup> to record TRPM7-mediated currents by preserving the intracellular milieu as intact as possible. As the result, we have found that continuous  $\text{Ca}^{2+}$  influx through spontaneously active TRPM7 channel facilitates both proliferation and erythroid differentiation of K562 cells most likely via  $\text{Ca}^{2+}$ -dependent

activation of the ERK-signalling.

## Results

### TRPM7 is a predominant TRP isoform expressed in K562

Both conventional and quantitative real-time RT-PCR experiments in K562 cells indicated that TRPM7 and TRPV2 are most predominantly expressed isoforms among all TRP family members (Figs.1A-C). Immunostaining of K562 cells with anti-TRPM7 antibody confirmed robust expression of TRPM7 protein, which is largely confined to the cell membrane (Fig.1D; see also Fig.5C).

Widespread expression of TRPV2 has been recognized in both myeloid and lymphoid leukaemia cells<sup>25</sup>. However, no such evidence has been obtained for TRPM7 despite its postulated ubiquity. Thus, TRPM7 may be an abundant TRP isoform uniquely expressed in K562 cell.

### K562 possesses robust basal Ca<sup>2+</sup> influx

TRPM7 is known as a spontaneously active channel permeant to Ca<sup>2+</sup> and Mg<sup>2+</sup> near the resting membrane potential<sup>10</sup>. Thus, it may act as a constitutive entry pathway for Ca<sup>2+</sup> and other divalent cations in K562 cells. Consistent with this expectation, removal of external Ca<sup>2+</sup> remarkably lowered the intracellular Ca<sup>2+</sup> concentration ([Ca<sup>2+</sup>]<sub>i</sub>) of K562, when monitored by fura-2 fluorescent imaging technique (Fig. 2A). Replacement of Ca<sup>2+</sup> with Ba<sup>2+</sup> partially restored fura-2 fluorescence (Figs.2A and C). In addition, the basal [Ca<sup>2+</sup>]<sub>i</sub> level of K562 cells was reversibly reduced by nonspecific cation channel blockers including SK&F96365 (SKF), 2-APB, ruthenium red (RR) and Gd<sup>3+</sup> at tens to hundred μM concentrations (Figs. 2B and D). **Notably, ruthenium red only slightly (by ~10%) reduced**

the basal  $[Ca^{2+}]_i$  level at the concentration ( $1\mu M$ ) reported to almost completely inhibit endogenous TRPV2 channels (Fig.2D; <sup>26</sup>). This suggests that these channels may contribute only marginally to basal  $Ca^{2+}$  influx in K562 cells.

### Spontaneously active inward current in K562

To confirm that external  $Ca^{2+}$ -dependence of basal  $[Ca^{2+}]_i$  observed above reflects the  $Ca^{2+}$  influx through spontaneously active TRPM7-channels, we next conducted a nystatin-perforated whole-cell recording in K562 cells under the conditions that would minimally disturb the intracellular homeostasis and metabolism. As demonstrated in Fig. 3A, a small but robust inward-going current ( $I_{spont}$ ) was recorded at -50 or -60mV without stimulation. The magnitude of  $I_{spont}$  was doubled in the absence of  $Ca^{2+}$  and  $Mg^{2+}$  (i.e.  $Na^+$  is the sole charge carrier) and totally abrogated when all cations were substituted by a large membrane-impermeant cation N-methyl, D-glucamine (NMDG). Furthermore, isotonic substitution of external cations with  $Ca^{2+}$ ,  $Mg^{2+}$  or  $Ba^{2+}$  also allowed measurable inward currents (Fig. 3C). The current-voltage (I-V) relationships of  $I_{spont}$  under various ionic conditions evaluated by a slow rising ramp voltage showed prominent outward-rectification with distinguishable shifts of the reversal potentials for  $Ca^{2+}$ ,  $Mg^{2+}$  and  $Ba^{2+}$  (Figs.3B and D). The relative permeability ratios of  $Ca^{2+}$ ,  $Ba^{2+}$  and  $Mg^{2+}$  to  $Na^+$  (calculated from these shifts; Fig.3D) are  $1.21 (\pm 0.15, n=7)$ ,  $0.77 (\pm 0.08, n=7)$ , and  $0.63 (\pm 0.01, n=10)$ , respectively. Although estimation of the cation permeability based on this method could be somewhat inaccurate with discrepancies to

previously reported values, the high  $\text{Ca}^{2+}$  permeability is a commonly observed feature of TRPM7 channel<sup>9,23,27</sup>. In support of this view, known blockers of TRPM7 such as  $\text{Gd}^{3+}$ , 2-APB and FTY720 (which inhibits TRPM7 relatively selectively)<sup>27-29</sup>, dose-dependently inhibited  $I_{\text{spont}}$  (Fig.4).

To more rigorously corroborate that the observed  $I_{\text{spont}}$  represents an endogenous TRPM7 activity, we next adopted the siRNA strategy specifically targeting TRPM7 (see the Methods). After substantial knockdown of TRPM7 expression by its specific siRNA induced by doxycycline [DXC(+); Figs. 5A and B], basal  $[\text{Ca}^{2+}]_i$  was much lower than control [i.e. without doxycycline; DXC(-)] and removal of  $\text{Ca}^{2+}$  from the bath produced only a marginal decrease in  $[\text{Ca}^{2+}]_i$  (filled circles in Fig.5C). Whole-cell recording also confirmed this observation with significantly reduced inward current density after TRPM7 knockdown (Fig.5D).

These results strongly suggest that both basal  $[\text{Ca}^{2+}]_i$  and  $I_{\text{spont}}$  reflect endogenous TRPM7 channel activities.

#### TRPM7 activity is functionally linked to K562 proliferation and erythroid differentiation.

In the final step, we explored the functional linkage of TRPM7 activity to the proliferation and erythroid differentiation of K562 cells. As shown in Figs. 6A and B, the growth rate of K562 was dependent on external  $\text{Ca}^{2+}$  concentration and significantly slowed down in the absence of  $\text{Ca}^{2+}$  in the culture medium [open circles in Fig.6A; DXC(-)0Ca in Fig.6B].. Strikingly, the proliferation of K562 almost completely ceased after siRNA knockdown of TRPM7 expression, which was not rescued by

increasing the extracellular  $\text{Ca}^{2+}$  concentration [filled circles in Fig.6A; DXC(+) in Fig.6B]. These results strongly suggest that basal  $\text{Ca}^{2+}$  influx is essential for K562 cell growth, the major part of which likely occurs through spontaneously active TRPM7 channels.

In a different series of experiments, we also investigated the possible contribution of TRPM7 activity to the differentiation of K562 cells into an erythroid lineage. As well known, many reagents triggering erythropoiesis can induce the synthesis of a fetal-form of haemoglobin in K562 cells (see the Introduction). We used hemin as a potent erythropoietic reagent and measured  $\gamma$ -globin as the differentiation marker, the essential subunit of fetal haemoglobin<sup>30</sup>. As shown in Figs.7A-C, 24h-treatment of K562 cells with hemin remarkably enhanced the expression of  $\gamma$ -globin without affecting TRPM7 activities (Suppl. Fig.1). Importantly, siRNA knockdown of TRPM7 expression, and chelation of  $\text{Ca}^{2+}$  by EGTA or addition of the TRPM7 blocker FTY720 in the culture medium all abolished hemin-induced  $\gamma$ -globin synthesis in K562 cells. Impairment of erythroid differentiation by these procedures was also confirmed by direct determination of haemoglobin concentration (Figs.7D and E).

Previous studies reported that the ERK signalling is crucial for both K562 proliferation and differentiation<sup>31-36</sup>. We therefore tested whether this signalling is involved in the observed differentiation of K562. As demonstrated in Fig.8, in response to hemin, the extent of ERK phosphorylation declined in hours but increased subsequently (in days). This observation is consistent with the finding of a previous study<sup>31</sup>. Notably, the knockdown of TRPM7 attenuated the extent ERK

phosphorylation not only in prior to hemin treatment, but also at the late phase (3 days) after hemin treatment [DXC(+) in Fig.8], suggesting that ERK activation may be involved in both proliferation and differentiation of K562 cells.

## Discussion

The present study has clearly shown that K562 cells constitutively express TRPM7 channels which likely serve as a spontaneously active  $\text{Ca}^{2+}$  entry pathway essential for maintaining basal  $[\text{Ca}^{2+}]_i$ . This is evidenced by a few key observations, i.e. robust expressions of TRPM7 mRNA and protein and identification of associated  $\text{Ca}^{2+}$ -transporting activities in K562 cells, and their effective elimination by treating with TRPM7-targeting siRNA or applying TRPM7 blockers such as FTY720. Importantly, the procedures compromising the  $\text{Ca}^{2+}$  influx through this channel, i.e. its blockers, siRNA knockdown, or removal of extracellular  $\text{Ca}^{2+}$ , all resulted in pronounced inhibition of both proliferation and erythroid differentiation by hemin. These results strongly suggest that a certain basal  $[\text{Ca}^{2+}]_i$  level is a prerequisite to the proliferation and differentiation of K562 cells, to which TRPM7-mediated  $\text{Ca}^{2+}$  influx indispensably contributes. Indeed, many other studies have reported that  $\text{Ca}^{2+}$  homeostasis maintained by basal  $\text{Ca}^{2+}$  influxes through various cell-specific  $\text{Ca}^{2+}$ -permeable channels are crucial for cellular functions and dysfunctions<sup>1,37</sup>.

The differentiation of erythromyeloid cells is regarded as a highly coordinated set of numerous signalling events which should occur in the right order at the right timing. A plethora of transcriptional regulators such as transcription factors, kinases, non-coding RNAs and DNA-binding proteins are involved therein<sup>20,38</sup>. There is good evidence that some steps of it depend critically on preceding elevations in  $[\text{Ca}^{2+}]_i$  or the presence of  $\text{Ca}^{2+}$  in the external milieu<sup>39,40</sup>. In apparent agreement, it is known that K562 cells express  $\text{Ca}^{2+}$ -mobilizing G-protein-coupled receptors whose stimulation lead

to  $[Ca^{2+}]_i$  elevation<sup>41</sup>. However, other studies provided seemingly contradictory observations. Albeit indirect evidence, it was shown that down-regulation of a voltage-dependent  $Ca^{2+}$  channel gene *Cacnad1* by mircoRNA-107 rather promotes K562 erythroid differentiation<sup>42</sup>. A hERG channel toxin BmKKx2, which is expected to depolarise the cell membrane, thereby reducing the driving force for transmembrane  $Ca^{2+}$  influx, was shown to retard the proliferation and facilitate the AraC-induced erythroid differentiation of K562 cells, respectively<sup>43,44</sup>. Furthermore, stimulation of  $Ca^{2+}$ -mobilizing glutamate receptor was found to enhance the proliferation of erythromyeloid stem cells including Meg-01, Set-2, and K562 cells, while its antagonist facilitated Meg-01 differentiation to megakaryocytes<sup>45</sup>. These results are consistent with the view that reduction of basal  $[Ca^{2+}]_i$  is a crucial event to cease proliferation and then initiate differentiating processes. In fact, our present study has also confirmed that the growth of K562 cells depended on the presence of extracellular  $Ca^{2+}$ , and interventions to decrease  $[Ca^{2+}]_i$  significantly decelerated it (Figs.6A and B). Nevertheless, the reduction of  $[Ca^{2+}]_i$  also impaired the haemoglobin synthesis induced by hemin (Fig.7). These confounding results may imply the involvement of inexplicably intricate  $Ca^{2+}$ -dependent mechanisms in the control of proliferation and differentiation. In this regard, one reconciling explanation could be that ERK activation follows variable, multi-phasic time courses in response to differentiating agents<sup>(31)</sup>; see below). It is well recognized that the Ras-ERK signalling occupies a central part in regulating cell proliferation and differentiation, where  $Ca^{2+}$ -dependent activation of Ras (e.g. through  $Ca^{2+}$ /calmodulin-mediated regulation of Ras-guanine-nucleotide-releasing factor or via complex

Pyk2-mediated signalling) may play a pivotal role<sup>46</sup>.

In erythropoiesis, there are disparate findings that both ERK activation and inhibition can promote differentiation of stem/progenitor cells into matured erythroid cells capable of producing haemoglobin. For example, while pharmacological inhibition of the Ras-Raf-Mek1-ERK signalling inhibits K562 proliferation leading to its erythroid differentiation, enhanced ERK activity by Ras overexpression is also shown to promote the differentiation<sup>31</sup>. Woessmann *et al.* (2004) investigated in detail this paradoxical commitment of ERK to erythroid differentiation in K562 cells by carefully chasing the time courses of ERK phosphorylation and concomitant haemoglobin synthesis. Their key findings are recapitulated as follows; in response to erythroid-differentiating agents, ERK phosphorylation declines in hours but thereafter follows differential time courses dependent on the differentiating agents used. While the phosphorylation remained decreased with butyrate or Ara-C, it increased again more than 24 hours later with cisplatin or hemin as the differentiating agent, and the late re-activation of ERK by cisplatin or hemin occurred at the same timing as the induction of haemoglobin synthesis. Moreover, MEK-1 inhibitors which decrease ERK phosphorylation induced the erythroid differentiation of K562 cells as well as inhibited hemin- or cisplatin-induced haemoglobin synthesis. The most plausible interpretation given to these findings is that inhibition of ERK activity is commonly involved in the initiation of erythroid differentiation, in other words, cessation of proliferation of K562 cells. In contrast, re-activation of ERK may be crucial for further forwarding the erythropoiesis by hemin or cisplatin. Our immunoblotting results on ERK

phosphorylation exactly match up with this view (Fig.8). In addition, it should be emphasized that TRPM7 channel activities (i.e.  $\text{Ca}^{2+}$  influx thereby) are essential to maintain the ERK activity both before and after hemin stimulation, respectively (Fig.8), so as to drive the proliferation and erythroid differentiation of K562 cells (Figs.6 and 7). This is the most important conclusion of the present study. At present, how such  $\text{Ca}^{2+}$  influx via TRPM7 channel would precisely divert the ERK-mediated signalling to either proliferation or differentiation remains unclear. Thus, it will need to be elucidated, in particular regarding the possible involvement of the Ras-GRP or Pyk2-mediated signalling<sup>46</sup>.

In summary, the present study has unveiled previously-unrecognized  $\text{Ca}^{2+}$ -dependent mechanisms via spontaneously active TRPM7 channels that likely regulate not only the proliferative potential but hemin-induced erythroid differentiation of a human erythromyeloid leukaemia cell line K562, in which ERK activation with different time courses may be involved. These results will further point to the possibility that any defective gating of TRPM7 channel due to hereditary and/or acquired causes might lead to human hematopoietic disorders such as anaemia and thrombocytopenia.

## **Materials and Methods**

### Cell culture

A human leukaemia cell line K562 was kindly provided by Prof. Y. Oyama at Department of Cellular Signaling, Tokushima University. K562 cells were suspended in a 5ml culture flask containing

RPMI1640 (RPMI) medium supplemented with 10% fetal bovine serum at 37°C in an incubator humidified and saturated with 5% CO<sub>2</sub>. Under these conditions, the number of K562 cells doubled per about two days, and the medium was changed afresh every 3-4 days.

### Electrophysiology

The equipment and protocols used for patch clamp experiments were essentially the same as those used previously<sup>23</sup>. Briefly, a high impedance, low noise patch clamp amplifier (Axopatch 1D, Axon Instruments, Union City, CA; EPC8, HEKA Elektronik, Lambrecht/Pflaz, Germany) in conjunction with an AD,DA converter (TL-1, Axon Instruments; LIH8+8, InstruTECH, Longmont, CO) was used to apply voltages to and obtain current signals from cells. The obtained signals were low-pass filtered at 1kHz and then stored in a computer hard disc after 2kHz digitization. The computer (Activa, IBM; Dell) was run by the dedicated software (pClamp v.6.03, Axon Instruments; Patchmaster v.2x90.1, HEKA Elektronik). For data analysis and illustration, Clampfit v.9.2 (Molecular Devices, San Jose, CA) and KaleidaGraph v.3.08 (Synergy Software, Reading, PA) were employed depending on the purposes. The input resistance of pipette was 2-4MΩ when filled with Cs<sup>+</sup>-based internal solution. About 80-90% of series resistance (5-7MΩ) was electronically compensated. The liquid junction potential arising at the interface of pipette and external solution (~6mV) was determined according to the method described by Neher<sup>47</sup>, and corrected when the current-voltage relationship was constructed. For long-lasting recording (>1min), MacLab/4 or PowerLab 4/25 (AD Instruments, **New**

South Wales, Australia) was used, with 50Hz low-pass filtering and 100Hz digitization. To minimize measuring errors arising from largely fluctuating currents, a 1s or longer-period of the current segment was average and subjected to analyses.

For nystatin-perforated recording, nystatin stock solution (Sigma; dissolved in DMSO at 50mM) was diluted 100-200 times in Cs<sup>+</sup>-based internal solution, and ultra-sonicated for 5-10min until the aggregates became totally dispersed. In each experiment, a patch electrode was briefly dipped in nystatin-free internal solution, back-filled with the one containing nystatin and tapped with fingers to mix thoroughly. After quickly equipping the pipette to a holder of a patch amplifier, it was pressed onto the cell and the giga-seal was formed by gentle suction. In a typical time course, the cell membrane was perforated by nystatin within 5min to lower the access resistance less than 20MΩ. All experiments were performed at room temperature.

Permeabilities of various external cations relative to Na<sup>+</sup> through TRPM7-mediated spontaneously active channels in K562 cells were evaluated under various bi-ionic conditions by their reversal potentials, the values of which were used to calculate the permeability ratio (P<sub>X</sub>/P<sub>Na</sub>) according to the modified Goldman-Hodgkin-Katz equation<sup>48</sup>:

$$P_X/P_{Na} = ([Na^+]_o/[X^{2+}]_o) \exp(\Delta E_{rev}F/RT) \quad \text{for monovalent cation (*)}$$

$$[\Delta E_{rev} = E_{rev(X)} - E_{rev(Na)}]$$

$$P_Y/P_{Na} = ([Na^+]_o/4[Y^{2+}]_o) \exp(\Delta E_{rev}F/RT) [1 + \exp(E_{rev(Y)}F/RT)] \quad \text{for divalent cation} \quad (*)$$

$$[\Delta E_{rev} = E_{rev(Y)} - E_{rev(Na)}]$$

where the activity coefficients of 0.77 and 0.524 were used for monovalent cations and divalent cations (100mM) respectively. The junction potentials of these solutions to the internal solution were measured separately and corrected.

### Ca<sup>2+</sup> imaging

After settling on a poly-L-lysine-coated cover slip, K562 cells were treated with fura-2AM (1 $\mu$ M) for 25-30min. Global changes in Ca<sup>2+</sup> concentration ([Ca<sup>2+</sup>]<sub>i</sub>) of these cells were monitored by using a digital fluorescence imaging system (Aquacosmos, Hamamatsu Photonics Co., Shizuoka, Japan). The cell was alternately illuminated by near-visible ultraviolet excitation lights of 340 and 380nm and emitted blue lights (filtered at 510 $\pm$ 10nm) were captured through an objective lens of a fluorescence microscope (200x magnification; IX70, Olympus, Tokyo, Japan) by a CCD camera (HISCA, Hamamatsu Photonics) and stored in a computer hard disc. Background fluorescence and auto-fluorescence from the cell were obtained before fura-2 loading and subtracted from the fluorescences obtained thereafter. To reduce the influence of quenching, the ratio of fluorescence intensities at 340 and 380nm excitation (F<sub>340</sub>/F<sub>380</sub>) was calculated according to the following equation and converted to [Ca<sup>2+</sup>]<sub>i</sub> values.

$$[Ca^{2+}]_i = \beta * (R - R_{min}) / (R_{max} - R)$$

Where R denotes the ratio ( $F_{340}/F_{380}$ ) of fluorescences at 340nm and 380nm ( $F_{340}$  and  $F_{380}$ , respectively). The values of  $\beta$ ,  $R_{min}$  and  $R_{max}$  were determined in vitro by using a commercial calibration kit (Molecular Probes, Eugene, OR), being 6.29, 0.83, 12.67, respectively.

#### Tetracyclin-inducible siRNA system

In earlier studies, the efficiency of oligonucleotide transfection into non-adherent cells was very low, and in addition, the knockdown of TRPM7 expression was found extremely cytotoxic. It was thus practically infeasible to create cell lines stably expressing TRPM7 siRNA. We therefore employed a modified tetracycline-inducible siRNA expression vector (prototype; pcDNA4/TO; Thermo Fisher Scientific, Waltham, MA) in which RNA-H1 promoter was inserted to improve the efficiency of siRNA expression (dubbed 'pTER<sup>+</sup>';<sup>49</sup>). We then subcloned into this vector the nucleotide sequence corresponding to the 170-188<sup>th</sup> N-terminal region of TRPM7 (TM7<sup>170-188</sup>: 5'-GTCTTGCCATGAAATACTC-3') that had previously proved to be an effective target for TRPM7 knockdown<sup>23</sup>, which is dubbed as pTER<sup>+</sup>-TM7-siRNA. More specifically, hairpin oligonucleotides containing the sense and anti-sense sequences of TM7<sup>170-188</sup> respectively (i.e. GATCCCGTCTTGCCATGAAATACTCTTCAAGAGAGAGTATTTTCATGGCAAGACTTTTT

GGAAA

and

AGCTTTTCCAAAAAGTCTTGCCATGAAATACTCTCTCTTGAAGAGTATTTTCATGGCAA

GACG, respectively) were dissolved at a concentration of  $1\mu\text{g}\ \mu\text{l}^{-1}$ ,  $2\mu\text{l}$  of which was mixed with  $46\mu\text{l}$  of annealing buffer (100mM K-acetate, 30mM HEPES-KOH pH7.4, 2mM Mg-acetate), and incubated successively at  $90^{\circ}\text{C}$  for 3min and at  $37^{\circ}\text{C}$  for one hour. pTER<sup>+</sup> was thoroughly digested by the restriction enzymes pair Bgl II/Hind III, electrophoresed on a 1% agarose gel, extracted by using a DNA extraction kit (GE Healthcare Piscataway, NJ), and finally ligated with the hybridized siRNA oligonucleotides by T4 DNA ligase (Thermo Fisher Scientific). The resultant ligation mixture was subjected to transformation, amplification and ampicillin-resistant colony selection with DH5 $\alpha$  competent *E. coli*. Successful incorporation of the siRNA oligonucleotides into the pTER<sup>+</sup> vector was confirmed by the resistance to EcoR I digestion, the site of which should be deleted after Bgl II/Hind III digestion. The final construct pTER<sup>+</sup>-TM7-siRNA was amplified on a large scale with the EndoFree Plasmid Maxi Kit (Qiagen, Hilden, Germany) for later use.

To construct a tetracycline-inducible expression system in K562 cells, we first introduced the tetracycline repressor (TetR) gene into the K562 genome with an improved electroporation technique (nucleofection; Amaxa BioSystems, Gaithersburg, MD). Briefly, K562 cells were centrifuged, re-suspended in a reaction solution containing  $2\mu\text{g}$  pcDNA6/TR plasmid, and transferred into a cuvette of an electroporator ('Nucleofector'). Both the reaction solution and electroporator were provided by the manufacturer. The optimized protocol for K562 (Nucleofector<sup>TM</sup> program No.T-16) was

employed to introduce the plasmid into K562 cells. After nucleofection, K562 cells were transferred into a culture flask filled with 10ml RPMI medium, and incubated for 48hrs, and subsequently, a 5 $\mu$ l of 1mM blasticidin S (Thermo Fisher Scientific) was added to the medium for selection. The amount of blasticidin S was increased in a step-by-step manner up to 10 $\mu$ l per 5ml. The cells that survived after blasticidin S selection (i.e. TetR<sup>+</sup>) were further transfected by nucleofection with pTER<sup>+</sup>-TM7-siRNA plasmid, and 24hrs thereafter, selected by adding zeocin (200-400 $\mu$ g ml<sup>-1</sup>: Thermo Fisher Scientific) in the medium to subclone K562 cells stably expressing both TetR and pTER<sup>+</sup>-TM7-siRNA (TetR<sup>+</sup>TM7<sup>+</sup>).

Expression of TRPM7-siRNA in TetR<sup>+</sup>TM7<sup>+</sup>-K562 cells was induced by adding doxycycline (0.1, 0.3, 1, 3, 10 $\mu$ M: Sigma) in the culture medium for 96hrs or longer. After this treatment, the cells were collected and subjected to RT-PCR and Western blot analyses (Figs.1 and 5).

#### Immunocytochemistry and immunoblotting

*Immunostaining of TRPM7 protein* : antisera against TRPM7 was raised by immunizing rabbits with a synthesized epitope corresponding to a common amino acid sequence between mouse (1813-1832) and human (1815-1834) TRPM7 C-termini: CRKLKLPDLKRNDYTPDKII (GenBank accession No. NO\_001157797.1 and NP\_001288141). K562 cells adherent on cover slips pre-coated with poly-L-lysine were fixed with 4% paraformaldehyde for 15min and permeablized with 0.2% Triton/PBS for 15min. After rinsing in PBS several times, the cells were incubated in 10% normal goat serum

(Jackson) for 1hr; 1:500 diluted TRPM7 antiserum at 4°C overnight; FITC-labelled anti-rabbit goat serum (Jackson Immuno Research Lab. Inc., West Grove, PA) for 1hr. Finally, the cells were embedded in Permafluor aqueous mounting solution (Immunon, Pittsburg, PA). Immunostained K562 cells were observed through a laser-scanning confocal microscope equipped with an argon/krypton laser source (FV500, Olympus). Emitted light (near 505nm) by 488 nm excitation was collected as 80-times magnified images and stored in a computer hard disc.

*Expression analysis by Western Blot* : untreated and treated K562 cells with doxycycline for 96hrs were collected. Cell pellets were directly resuspended in sodium dodecyl sulfate (SDS) sample buffer (62.5 mM Tris-HCl pH 6.8, 2% SDS, 10% glycerol, 50 mM dithiothreitol (DTT), 0.1% bromophenol blue), incubated for 5 minutes at 95°C, cooled on ice for 5 minutes and stored at -20°C until further use. The denaturate was then electrophoresed on an acrylamide gel (at 40mA for 1hr respectively) and blotted on a PVDF membrane. To prevent detecting nonspecific bands, the membrane was shaken in 10%BSA-containing Tris buffered saline with Tween® 20 (TBS-T) or phosphate buffered saline with Tween® 20 (PBS-T) for 1hr and rinsed with TBS-T or PBS-T; thereafter, allowed to react with either 1:500-diluted TRPM7 antiserum, 1:2000-diluted Phospho-p44/42 MAPK (P-eErk1/2; 4379, Cell Signaling, Boston, MA) or 1:2000-diluted p44/42 MAPK (Erk1/2; 4695, Cell Signaling) (in TBS-T or PBS-T) at 4°C overnight; subsequently with anti-rabbit goat IgG (Santa Cruz Biotechnology, Santa Cruz, CA) for 1hr after rinsing with TBS-T or PBS-T. After these procedures, the chemiluminescence of the membrane which was treated with the Western Lightning

Chemiluminescence Reagent Plus (Perkin Elmer, Boston, MA) was detected by the LAS system (LAS-3000, Fujifilm, Tokyo, Japan) and analysed with the Image Gauge software (Fujifilm).  $\beta$ -actin or  $\alpha$ -tubulin was taken as a reference, for which mouse monoclonal anti- $\beta$ -actin antibody (AC-15, Abcam, Cambridge, UK), or  $\alpha$ -tubulin antibody (T6074, Sigma Aldrich), anti-mouse IgG, and horseradish peroxidase linked whole antibody (from sheep) (GE Healthcare) were used.

#### Reverse transcription polymerase reaction (RT-PCR) and real-time PCR

Total RNA (about 1 $\mu$ g) was extracted from about a million of K562 cells with the Total RNA extraction Kit (RNeasy Minikit, Qiagen) and reverse-transcribed (in a 10 $\mu$ l scale) by SuperScriptII (Thermo Fisher Scientific) with a randomized or an oligo-dT primer to obtain the first strand DNA. PCR amplification (in a 20 $\mu$ l scale) was performed with a heat-resistant DNA polymerase (PrimeSTAR GXL, Takara) in a thermal cycler (Biometra, Gottingen, Germany) according to the following protocol ; denaturation at 94°C for 2min followed by 17-35 cycles of: denaturation (94°C, 10s), annealing (60°C, 10s) and extension (72°C, 30s). The PCR amplicons were electrophoresed in a 1.2-1.5% agarose gel for 45-60min, hybridized with ethidium bromide (Nacalai Tesque, Kyoto, Japan) or GelRed<sup>TM</sup> (Biotium, Fremont, CA) and visualized by ultraviolet or Blue/Green LED light, respectively. The densitometry analysis of electrophoresed PCR amplicons was performed using the ImageJ software (Public domain, NIH, USA)

The sequences of PCR primer pairs are as follows (5' to 3', sense / antisense) ;

TRPM1: GGGGATGCCTTGAAAGACCA / GCCAAGCTCAGCTGATCTGGA

TRPM2: CTTCCGGGAAGGCAAGGATGGT / GAGGCTCACTCCCTGCACGTT

TRPM3: GAGGAGACCATGTCCCCAACTT / GAGTAGCTGTTGGCGCGCT

TRPM4: GTCATCGTGAGCAAGATGATGAA / GTCCACCTTCTGGGACGTGC

TRPM5: CAAGTGTGACATGGTGGCCATCTT / GCTCAGGTGGCTGAGCAGGAT

or GTGACTGTGTTCTGGGGAA / GACCAGCCAGTTGGCATAGA

TRPM6: GAGGAGATGGATGGGGGCCT / GGTCCAGTGAGAGAAAGCCAACAT

TRPM7: CCATACCATATTCTCCAAGGTTC / CATTCTCTTCAGATCTGGAAGTT

TRPM8: GAAGGCACCCAGATCAACCAA / GAGCCTTCCACCACCACACA

or CTTCGTGGTCTTCTCCTGGAA / CATGGCCAGGTAGGGCTC

GAPDH: ATCACCATCTTCCAGGAGCGAG / TGGCATGGACTGTGGTCATG

or GGTGAAGGTCGGAGTCAACG / CAAAGTTGTCATGGATGACC

$\gamma$ -globin: GGCAACCTGTCCTCTGCCTC / GAAATGGATTGCCAAAACGG

In separate experiments, quantitative real-time PCR was performed for all other TRP superfamily members in addition to those of TRPM subfamily with primer pairs; (5' to 3'; sense / antisense).

TRPC1: GCGTAGATGTGCTTGGGAGAAA / GCTCTCAGAATTGGATCCTCCTCT

TRPC2: GCTGGCCAAGCTGGCCAA / CATCCTCACTGGCCAGCGAGA

TRPC3: CCTCTCAGCACATCGACAGGT / GAACACAAGCAGACCCAGGAAGA

TRPC4: CAAGCTTCTAACCTGCATGACCA / CCAAATATTGACCAAAACAGGGA

TRPC5: CATCCCAGTGGTGCGGAAGA / CCTAAGTGGGAGTTGGCTGTGAA

TRPC6: GAGGAGGAGCGCTTCCTGGACT / GCCTTCAAATCTGTCAGCTGCA

TRPC7: CCAGGTGGTCCTCTGCGGAA / GGCTCAGACTTGGACGGTGGT

TRPV1: GAAGATCGGGGTCTTGGCCTA / CTCACTGTAGCTGTCCACAAACAAA

TRPV2: GACGTGCCTGATGAAGGCTGT / CTGGTGTGGGTTCTCCAGGA

TRPV3; AGTGGCAACTGGGAGCTGG / GGGTCAGGGTGATGTTGTAGAAGA

TRPV4: GTGCCTGGGCCCAAGAAA / GGGCAGCTCCCCAAAGTAGAA

TRPV5: CTCACCCCCTTCAAGCTGGCT / CCCAGCATCTGGAATCCTCG

TRPV6: GCCGAGATGAGCAGAACCTGCT / GTCTGGTCCAGGATCTGGCGA

Real time PCR was implemented by using the "Line-Gene" Fluorescent Quantitative Detection System (BioFlux, Tokyo, Japan) or Smart Cycler System II (Cepheid, Sunnyvale, CA) with the 1st strand DNA and PCR reagent (TakaraBio Inc., Shiga, Japan or TOYOBO, Osaka, Japan) according to the manufacturer's instructions. Data analysis was made with the software dedicated to the respective systems.

### Cell counting assay

K562 cells ( $5 \times 10^4$ ) were replated in a 6cm dish and incubated in  $\text{Ca}^{2+}$ -free, 10% serum-added RPMI medium for 3 days with or without  $10 \mu\text{g ml}^{-1}$  doxycycline. Thereafter, an aliquot ( $1 \mu\text{l}$ ) of the Acridine Orange / Propidium Iodide (AO/PI) Cell Viability Kit (Logos Biosystems, Republic of Korea) was added to each  $100 \mu\text{l}$  of samples. After the incubation at room temperature for 10 minutes, the cell staining solution was loaded onto the counting slide of Countess and the loaded cell sample images were acquired from CountessII-FL (Thermo Fisher Scientific). The cells positive for AO were taken viable and counted to calculate the proliferation rate.

### Quantitation of haemoglobin synthesis

To assess haemoglobin synthesis, K562 cells were stimulated with hemin ( $40 \mu\text{M}$ ) for three days, and then centrifuged and washed with PBS. The resultant cell pellet was resuspended in lysis buffer ( $100 \text{ mM}$  potassium phosphate pH 7.8, 0.2% Triton X-100) and incubated 10 minutes at room temperature. After precipitating cellular debris by centrifugation, the supernatant was collected and the quantity of haemoglobin contained in it was determined using the plasma haemoglobin colorimetric assay kit, according to the manufacturer's instructions (Cayman Chemical, Ann. Arbor, MI). The haemoglobin concentration was calculated as  $\text{g dl}^{-1}$  by dividing the Hb quantity by the number of cells measured by the Countess II-FL (Thermo Fisher Scientific).

## Solutions

The composition of solutions used were as follows.

Extracellular (bath) solution (physiological saline solution: PSS) (in mM): 140 Na<sup>+</sup>, 5 K<sup>+</sup>, 1.2 Mg<sup>2+</sup>, 2 Ca<sup>2+</sup>, 151.4 Cl<sup>-</sup>, 5 glucose, 10 HEPES (adjusted at pH7.4 with Tris<sup>+</sup>). Drugs were dissolved in PSS and topically applied through a home-made, fast solution change device (solenoid-valve driven 'Y-tube'). To prepare Ca<sup>2+</sup>-deficient external solution, 0.5mM EGTA was added to thoroughly chelate residual Ca<sup>2+</sup>. **In some experiments measuring Ba<sup>2+</sup> fluorescence (Figs.2A and 2C), nominally Ca<sup>2+</sup>-free rather than 0.5mM EGTA-containing external solution was used.**

Ca<sup>2+</sup>, Mg<sup>2+</sup>-free Na<sup>+</sup> external solution consisted of (mM): 150 Na<sup>+</sup>, 150 Cl<sup>-</sup>, 1 EDTA, 5 glucose, 10HEPES; Ca<sup>2+</sup>, Ba<sup>2+</sup> or Mg<sup>2+</sup> external solutions (mM) ; 100 Ca<sup>2+</sup>, Ba<sup>2+</sup> or Mg<sup>2+</sup>, 200 Cl<sup>-</sup>, 5 glucose, 10 HEPES (adjusted at pH7.4 with Tris<sup>+</sup>).

Cs-based internal solution for conventional and nystatin-perforated whole-cell recordings contained (mM) : 140 Cs<sup>+</sup>, 20 Cl<sup>-</sup>, 120 aspartate<sup>-</sup>, 5BAPTA, 1.5Ca<sup>2+</sup>, 10 glucose, 10HEPES (adjusted at pH7.4 with Tris<sup>+</sup>).

## Material and drugs

N-methyl, D-glucamine (NMDG), adenosine 1,4,5-trisphosphate (ATP), 1,2-bis(o-aminophenoxy)etane-N,N,N',N'-tetraacetic acid (BAPTA), 1-(4-aminobenzyl) ethylenediamine-N,N,N',N'-tetra acetic acid (AM-EDTA), ethyleneglycol-bis(β-aminoethyl)- N,N,N',N'- tetra acetic

acid (EGTA), ethylenediamine-N,N,N',N'-tetra acetic acid (EDTA), hemin, HEPES and GdCl<sub>3</sub> were purchased from Sigma and SK&F96365, 2-aminoethoxydiphenyl borate (2-APB) and ruthenium red (RR) from Calbiochem, and FTY720 from Cayman Chemical, respectively.

pTER<sup>+</sup> was kindly provided by Dr. M. van de Wetering (Hubrecht Laboratory, Center for Biomedical Genetics, Netherlands).

### Statistical evaluation

All data shown in figures are expressed as mean  $\pm$  s.e.m. Statistical significance between different groups was assessed by Student's paired **or unpaired** *t*-test for single comparison and two-way ANOVA followed by Tukey's test for multiple comparison with the aid of a commercial software JMP v.12.2 (SAS Institute Inc., Cary, NC).

**Acknowledgements**

We cordially thank for Professors Yushi Ito (Kumamoto Health Science University) and Hideki Sumimoto (Graduate School of Medical Sciences, Kyushu University) for their pertinent advice and generous help during the early stage of this study. Preliminary part of this work was performed by C.U. and R.I at Department of Pharmacology, Graduate School of Medical Sciences, Kyushu University.

**Conflict of Interest:** None

## References

1. Berridge MJ, Bootman MD, Roderick HL. Calcium signalling: dynamics, homeostasis and remodelling. *Nat Rev Mol Cell Biol.* 2003;4(7):517-529.
2. Means AR. Calcium, calmodulin and cell cycle regulation. *FEBS Lett.* 1994;347(1):1-4.
3. Whitfield JF, Bird RP, Chakravarthy BR, Isaacs RJ, Morley P. Calcium-cell cycle regulator, differentiator, killer, chemopreventor, and maybe, tumor promoter. *J Cell Biochem Suppl.* 1995;22:74-91.
4. Berridge MJ. Calcium signalling and cell proliferation. *Bioessays.* 1995;17(6):491-500.
5. Borowiec AS, Bidaux G, Pigat N, Goffin V, Bernichtein S, Capiod T. Calcium channels, external calcium concentration and cell proliferation. *Eur J Pharmacol.* 2014;739:19-25.
6. Deliot N, Constantin B. Plasma membrane calcium channels in cancer: Alterations and consequences for cell proliferation and migration. *Biochimica et biophysica acta.* 2015;1848(10 Pt B):2512-2522.
7. Ryazanova LV, Dorovkov MV, Ansari A, Ryazanov AG. Characterization of the protein kinase activity of TRPM7/ChaK1, a protein kinase fused to the transient receptor potential ion channel. *J Biol Chem.* 2004;279(5):3708-3716.
8. Visser D, Middelbeek J, van Leeuwen FN, Jalink K. Function and regulation of the channel-kinase TRPM7 in health and disease. *Eur J Cell Biol.* 2014;93(10-12):455-465.
9. Monteilh-Zoller MK, Hermosura MC, Nadler MJ, Scharenberg AM, Penner R, Fleig A. TRPM7 provides an ion channel mechanism for cellular entry of trace metal ions. *J Gen Physiol.* 2003;121(1):49-60.
10. Nadler MJ, Hermosura MC, Inabe K, et al. LTRPC7 is a Mg.ATP-regulated divalent cation channel required for cell viability. *Nature.* 2001;411(6837):590-595.
11. Aarts M, Iihara K, Wei WL, et al. A key role for TRPM7 channels in anoxic neuronal death. *Cell.* 2003;115(7):863-877.
12. Langeslag M, Clark K, Moolenaar WH, van Leeuwen FN, Jalink K. Activation of TRPM7 channels by phospholipase C-coupled receptor agonists. *J Biol Chem.* 2007;282(1):232-239.
13. Abed E, Moreau R. Importance of melastatin-like transient receptor potential 7 and cations (magnesium, calcium) in human osteoblast-like cell proliferation. *Cell Prolif.* 2007;40(6):849-865.
14. Du J, Xie J, Zhang Z, et al. TRPM7-mediated Ca<sup>2+</sup> signals confer fibrogenesis in human atrial fibrillation. *Circ Res.* 2010;106(5):992-1003.
15. Jin J, Wu LJ, Jun J, et al. The channel kinase, TRPM7, is required for early embryonic development. *Proc Natl Acad Sci U S A.* 2012;109(5):E225-233.
16. Clark K, Langeslag M, van Leeuwen B, et al. TRPM7, a novel regulator of actomyosin contractility and cell adhesion. *EMBO J.* 2006;25(2):290-301.
17. Schappe MS, Szteyn K, Stremaska ME, et al. Chanzyme TRPM7 Mediates the Ca<sup>(2+)</sup> Influx Essential for Lipopolysaccharide-Induced Toll-Like Receptor 4 Endocytosis and Macrophage Activation. *Immunity.* 2018;48(1):59-74 e55.

18. Lozzio BB, Lozzio CB. Properties and usefulness of the original K-562 human myelogenous leukemia cell line. *Leuk Res.* 1979;3(6):363-370.
19. Villeval JL, Pelicci PG, Tabilio A, et al. Erythroid properties of K562 cells. Effect of hemin, butyrate and TPA induction. *Exp Cell Res.* 1983;146(2):428-435.
20. Tsiftoglou AS, Pappas IS, Vizirianakis IS. Mechanisms involved in the induced differentiation of leukemia cells. *Pharmacol Ther.* 2003;100(3):257-290.
21. Heise N, Palme D, Misovic M, et al. Non-selective cation channel-mediated Ca<sup>2+</sup>-entry and activation of Ca<sup>2+</sup>/calmodulin-dependent kinase II contribute to G2/M cell cycle arrest and survival of irradiated leukemia cells. *Cell Physiol Biochem.* 2010;26(4-5):597-608.
22. Semenova SB, Fomina AF, Vassilieva IO, Negulyaev YA. Properties of Mg(2+)-dependent cation channels in human leukemia K562 cells. *J Cell Physiol.* 2005;205(3):372-378.
23. Hanano T, Hara Y, Shi J, et al. Involvement of TRPM7 in cell growth as a spontaneously activated Ca<sup>2+</sup> entry pathway in human retinoblastoma cells. *J Pharmacol Sci.* 2004;95(4):403-419.
24. Horn R, Marty A. Muscarinic activation of ionic currents measured by a new whole-cell recording method. *J Gen Physiol.* 1988;92(2):145-159.
25. Morelli MB, Liberati S, Amantini C, et al. Expression and function of the transient receptor potential ion channel family in the hematologic malignancies. *Curr Mol Pharmacol.* 2013;6(3):137-148.
26. Pottosin I, Delgado-Enciso I, Bonales-Alatorre E, Nieto-Pescador MG, Moreno-Galindo EG, Dobrovinskaya O. Mechanosensitive Ca(2+)-permeable channels in human leukemic cells: pharmacological and molecular evidence for TRPV2. *Biochimica et biophysica acta.* 2015;1848(1 Pt A):51-59.
27. Li M, Jiang J, Yue L. Functional characterization of homo- and heteromeric channel kinases TRPM6 and TRPM7. *J Gen Physiol.* 2006;127(5):525-537.
28. Qin X, Yue Z, Sun B, et al. Sphingosine and FTY720 are potent inhibitors of the transient receptor potential melastatin 7 (TRPM7) channels. *Br J Pharmacol.* 2013;168(6):1294-1312.
29. Chubanov V, Schafer S, Ferioli S, Gudermann T. Natural and Synthetic Modulators of the TRPM7 Channel. *Cells.* 2014;3(4):1089-1101.
30. Dean A, Ley TJ, Humphries RK, Fordis M, Schechter AN. Inducible transcription of five globin genes in K562 human leukemia cells. *Proc Natl Acad Sci U S A.* 1983;80(18):5515-5519.
31. Woessmann W, Zwanzger D, Borkhardt A. ERK signaling pathway is differentially involved in erythroid differentiation of K562 cells depending on time and the inducing agent. *Cell Biol Int.* 2004;28(5):403-410.
32. Witt O, Sand K, Pekrun A. Butyrate-induced erythroid differentiation of human K562 leukemia cells involves inhibition of ERK and activation of p38 MAP kinase pathways. *Blood.* 2000;95(7):2391-2396.
33. Kucukkaya B, Arslan DO, Kan B. Role of G proteins and ERK activation in hemin-induced erythroid differentiation of K562 cells. *Life Sci.* 2006;78(11):1217-1224.
34. Sawafuji K, Miyakawa Y, Kizaki M, Ikeda Y. Cyclosporin A induces erythroid differentiation of

- K562 cells through p38 MAPK and ERK pathways. *Am J Hematol.* 2003;72(1):67-69.
35. Kang CD, Do IR, Kim KW, et al. Role of Ras/ERK-dependent pathway in the erythroid differentiation of K562 cells. *Exp Mol Med.* 1999;31(2):76-82.
  36. Whalen AM, Galasinski SC, Shapiro PS, Nahreini TS, Ahn NG. Megakaryocytic differentiation induced by constitutive activation of mitogen-activated protein kinase kinase. *Mol Cell Biol.* 1997;17(4):1947-1958.
  37. Bagur R, Hajnoczky G. Intracellular Ca(2+) Sensing: Its Role in Calcium Homeostasis and Signaling. *Mol Cell.* 2017;66(6):780-788.
  38. Hattangadi SM, Wong P, Zhang L, Flygare J, Lodish HF. From stem cell to red cell: regulation of erythropoiesis at multiple levels by multiple proteins, RNAs, and chromatin modifications. *Blood.* 2011;118(24):6258-6268.
  39. Levenson R, Housman D, Cantley L. Amiloride inhibits murine erythroleukemia cell differentiation: evidence for a Ca<sup>2+</sup> requirement for commitment. *Proc Natl Acad Sci U S A.* 1980;77(10):5948-5952.
  40. Tsiftoglou AS, Mitrani AA, Housman DE. Procaine inhibits the erythroid differentiation of MEL cells by blocking commitment: possible involvement of calcium metabolism. *J Cell Physiol.* 1981;108(3):327-335.
  41. Thomas CP, Dunn MJ, Mattera R. Ca<sup>2+</sup> signalling in K562 human erythroleukaemia cells: effect of dimethyl sulphoxide and role of G-proteins in thrombin- and thromboxane A<sub>2</sub>-activated pathways. *Biochem J.* 1995;312 ( Pt 1):151-158.
  42. Ruan J, Liu X, Xiong X, et al. miR107 promotes the erythroid differentiation of leukemia cells via the downregulation of Cacna2d1. *Mol Med Rep.* 2015;11(2):1334-1339.
  43. Ma J, Hu Y, Guo M, Huang Z, Li W, Wu Y. hERG potassium channel blockage by scorpion toxin BmKKx2 enhances erythroid differentiation of human leukemia cells K562. *PLoS One.* 2013;8(12):e84903.
  44. Zhang D, Cho E, Wong J. A critical role for the co-repressor N-CoR in erythroid differentiation and heme synthesis. *Cell Res.* 2007;17(9):804-814.
  45. Kamal T, Green TN, Morel-Kopp MC, et al. Inhibition of glutamate regulated calcium entry into leukemic megakaryoblasts reduces cell proliferation and supports differentiation. *Cell Signal.* 2015;27(9):1860-1872.
  46. Cullen PJ, Lockyer PJ. Integration of calcium and Ras signalling. *Nat Rev Mol Cell Biol.* 2002;3(5):339-348.
  47. Neher E. Correction for liquid junction potentials in patch clamp experiments. *Methods Enzymol.* 1992;207:123-131.
  48. Lewis CA. Ion-concentration dependence of the reversal potential and the single channel conductance of ion channels at the frog neuromuscular junction. *J Physiol.* 1979;286:417-445.
  49. van de Wetering M, Oving I, Muncan V, et al. Specific inhibition of gene expression using a stably integrated, inducible small-interfering-RNA vector. *EMBO Rep.* 2003;4(6):609-615.

**Legends to Figures**

Figure 1. Detection of TRPM7 expression in K562 cells.

A: Conventional RT-PCR. B: representative amplification curves of various TRP isoforms constructed by real-time PCR. C: Summary of the results of real-time PCR (n=5). TRPM7 and TRPV2 are most abundantly expressed among TRP superfamily members. In B, each amplification curve is plotted according to the calibration calculated for  $\beta$ -actin. The ordinates of histograms in C indicate the relative expression of respective TRP isoforms (normalized to GAPDH expression). D: Immunocytochemical staining with FITC-labelled anti-TRPM7 antibody. DIC image (upper) and immunofluorescence to TRPM7 (lower).

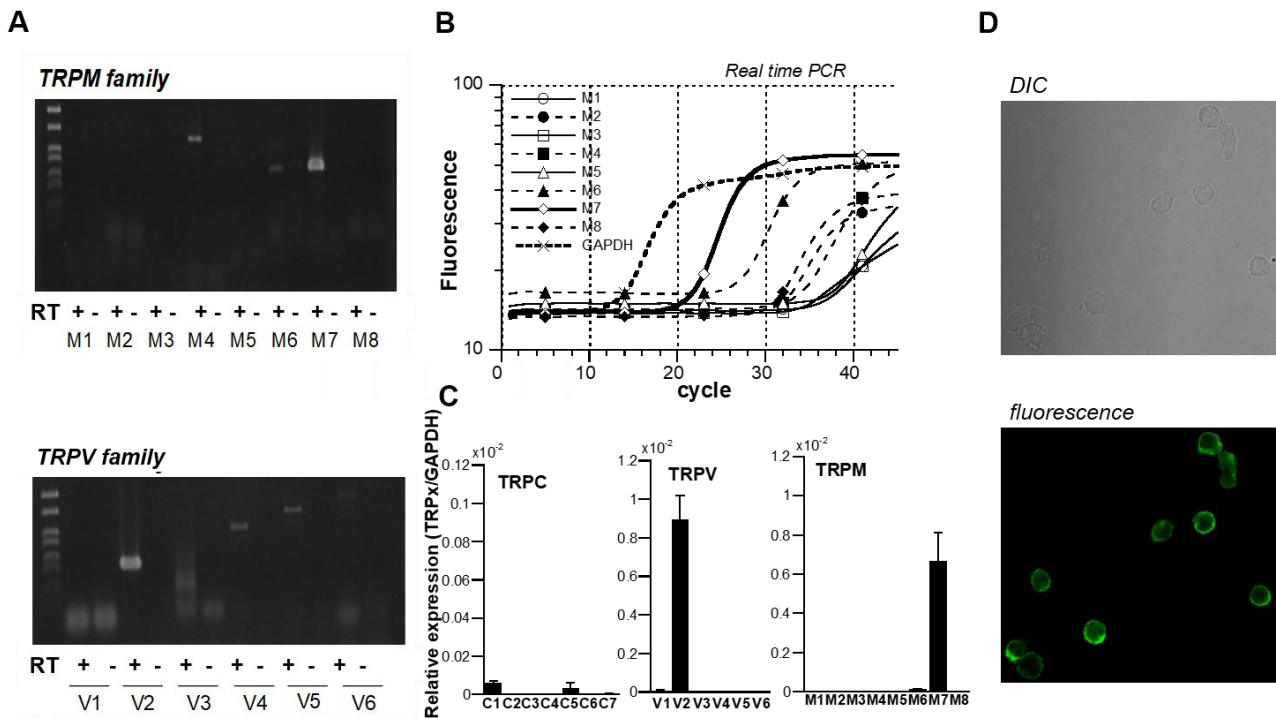


Figure 2. Ionic and pharmacological properties of basal  $\text{Ca}^{2+}$  influx in K562 cells.

Fura-2 fluorescence imaging. A: switching from PSS (2mM  $\text{Ca}^{2+}$  present: 2Ca) to  $\text{Ca}^{2+}$ -free PSS lowered basal  $\text{Ca}^{2+}$  level, and subsequent application of 0.5mM  $\text{Ca}^{2+}$  (0.5Ca) or 5mM  $\text{Ba}^{2+}$  (5Ba) partially recovered it. B: SK&F96365 (SKF), 2-aminoethoxydiphenyl borate (2-APB), ruthenium red (RR) and  $\text{Gd}^{3+}$  effectively inhibited basal  $\text{Ca}^{2+}$  influx at the concentrations indicated. Note: in A, 'Ca-free' denotes nominally  $\text{Ca}^{2+}$ -free external solution, while in B, 'Ca-free (0.5EGTA)' denotes that 0.5mM EGTA is added in Ca-free external solution. The numbers of cells simultaneously tested (n) are shown in panel A and B. C; Changes in the fluorescence ratio ( $F_{340}/F_{380}$ ) by switching from Ca-free to 0.5mM  $\text{Ca}^{2+}$  (0.5Ca) or 5mM  $\text{Ba}^{2+}$  (5Ba)-containing bath solutions are normalized to the ratio difference between Ca-free and 2mM Ca-containing bath solutions as shown in A are averaged. D; fractional reductions of  $F_{340}/F_{380}$  ratio (normalized to the ratio difference between Ca-free and 2mM Ca-containing bath solutions) after application of drugs (for abbreviations, see above). Data obtained from experiments such as shown in B are averaged. The numbers in parentheses in C and D denote those of independent imaging experiments, each being derived from the same batches of 17- 68 K562 cells. \*\* indicates  $P < 0.01$  with Tukey's multiple comparison test. Only statistically significant results are shown.

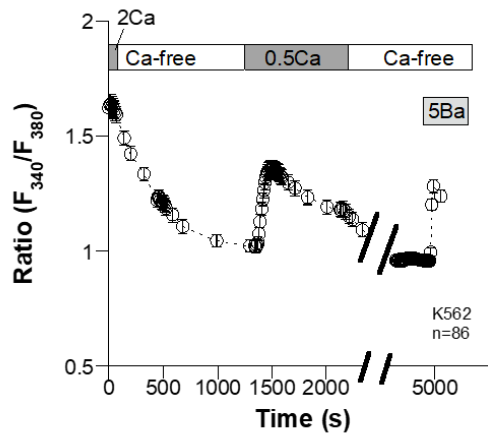
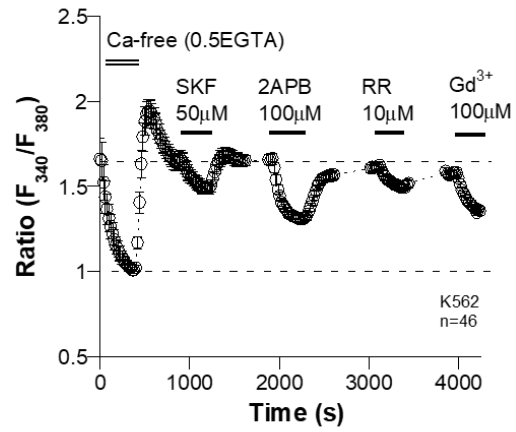
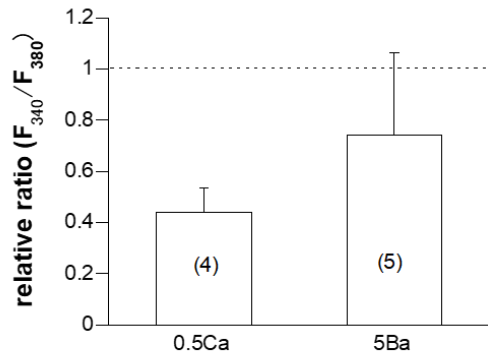
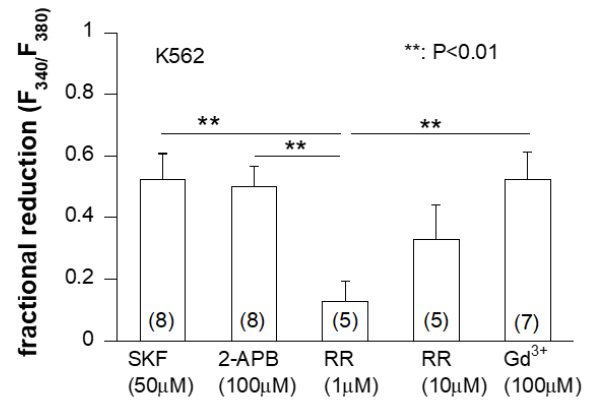
**A****B****C****D**

Fig.3 Spontaneous inward current ( $I_{\text{spont}}$ ) and its divalent cation permeability in K562 cells

A ; An actual trace of  $I_{\text{spont}}$  recorded from a K562 cell by the nystatin-perforated whole-cell patch clamp (holding: -60mV). Bath solution: PSS (2mM  $\text{Ca}^{2+}$  present). Pipette solution:  $\text{Cs}^+$ -based internal solution. At respective bars, the following solutions were rapidly applied through the 'Y-tube' device; NMDG (150mM NMDG-Cl); 100Mg (100mM  $\text{MgCl}_2$ ); 100Ca (100mM  $\text{CaCl}_2$ ); 100Ba (100mM  $\text{BaCl}_2$ ); 0Ca0Mg (150mM Na without divalent cations). Vertical deflections indicate the currents induced by ascending ramp voltages (-120 - +100mV, 1s). B; representative current-voltage (mp) relationships of  $I_{\text{spont}}$  evaluated by ramp voltages under various ionic conditions as shown in A. C; fold-changes of  $I_{\text{spont}}$  amplitude under various ionic conditions as shown in A. The amplitudes of  $I_{\text{spont}}$  (at -50mV) under various ionic conditions (0Ca0Mg, 100Ca, 100Ba or NMDG) are normalized to that in PSS, and averaged. D; averaged shifts of the reversal potential ( $E_{\text{rev}}$ ) of  $I_{\text{spont}}$  under various ionic conditions relative to the  $E_{\text{rev}}$  in 0Ca0Mg (i.e. 150mM NaCl) are shown. The numbers in parentheses in C and D denote those of independent K562 cells tested. \*, \*\* and \*\*\* respectively indicate P values of <0.05, <0.01 and <0.001 with Tukey's multiple comparison test. Only statistically significant results are shown.



Fig.4 Pharmacological properties of  $I_{\text{spont}}$  in K562 cells.

A, B; actual traces showing the inhibitions of  $I_{\text{spont}}$  by TRPM7 channel blockers,  $\text{Gd}^{3+}$  and FTY720, respectively. The recording conditions were the same as in Fig.3. C; concentration-dependent inhibition of  $I_{\text{spont}}$  by 10, 100 and 1000 $\mu\text{M}$   $\text{Gd}^{3+}$ . The fraction of  $I_{\text{spont}}$  remaining after the inhibition (fractional current) is averaged and illustrated. D; inhibitory effects of 2-APB on the current density of  $I_{\text{spont}}$ . E; relative inhibitions of  $I_{\text{spont}}$  by FTY720 at 1 and 10 $\mu\text{M}$ . The fraction of  $I_{\text{spont}}$  remaining after the inhibition (fractional current) is averaged and illustrated. The numbers in parentheses indicate the numbers of K562 cells tested. \*:  $P < 0.05$  with Dunnett' test vs. control (i.e. before application of drugs) (C and E) or unpaired Student *t*-test (D).

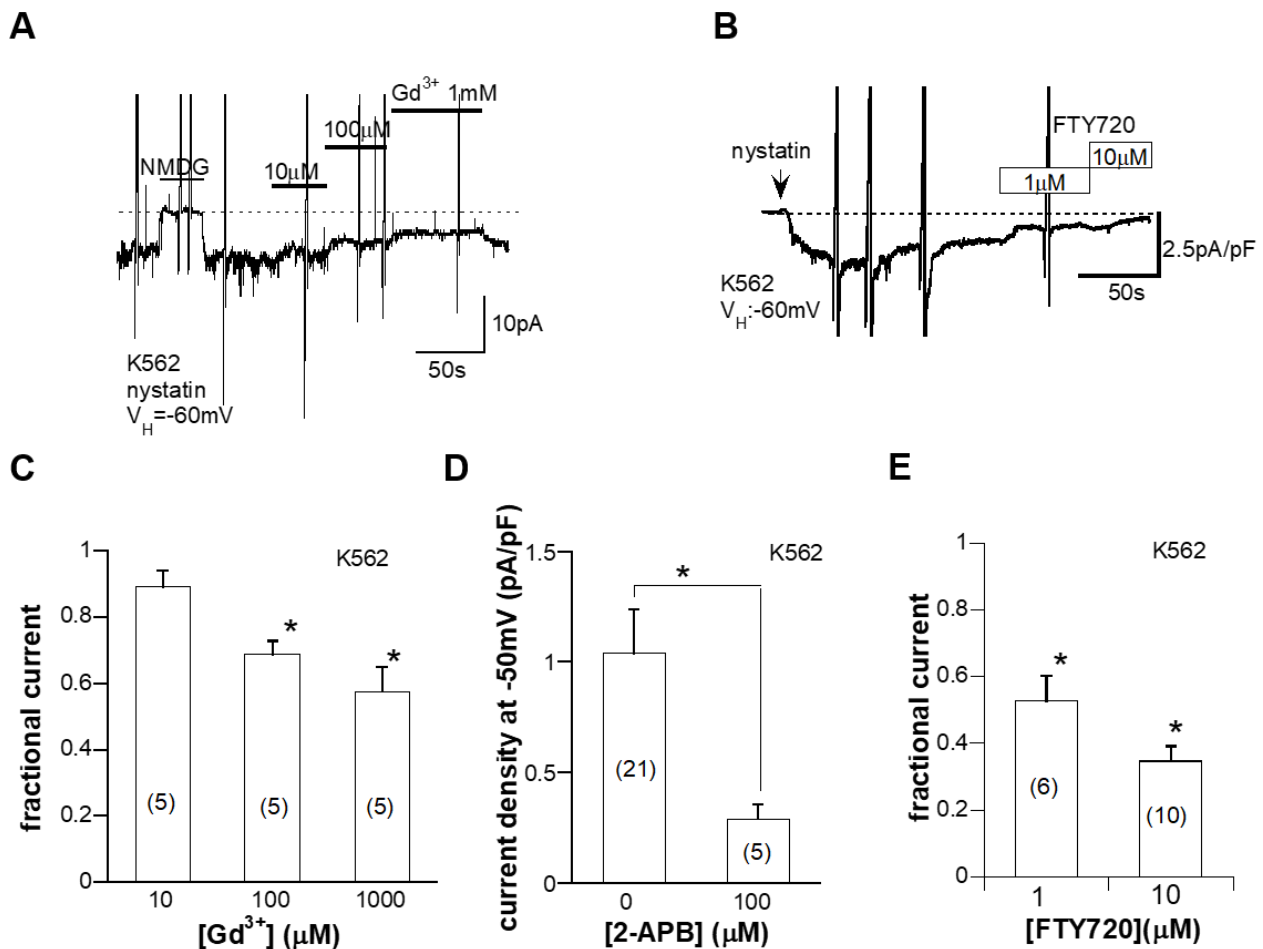


Fig.5 siRNA knockdown of TRPM7 channel abrogates  $\text{Ca}^{2+}$  influx and  $I_{\text{spont}}$  in K562 cells.

A; detection of TRPM7 transcripts (398bp) by conventional RT-PCR. Ten  $\mu\text{M}$  doxycycline (DXC) almost completely eliminated TRPM7 mRNA expression. B; immunoblots of K562 protein extracts by TRPM7 antibody. Doxycycline concentration-dependently (0.1-10 $\mu\text{M}$ ) reduced TRPM7 protein expression. **The results shown in A and B are representative of 3 independent experiments.** C; fura-2  $\text{Ca}^{2+}$  fluorescence imaging from untreated ([DXC(-)] and 10 $\mu\text{M}$  doxycycline-treated [DXC(+)] K562 cells stably expressing *tet*-inducible TRPM7-specific siRNA (siTRPM7). n=36 and 26, respectively. D; density of  $I_{\text{spont}}$  recorded by conventional whole-cell recording from untreated ([DXC(-)] and 10 $\mu\text{M}$  doxycycline-treated [DXC(+)] K562 cells stably expressing siTRPM7. To facilitate the induction of TRPM7 currents, ATP and  $\text{Mg}^{2+}$  were absent **in** the patch pipette. The numbers of cells tested are shown in parentheses.

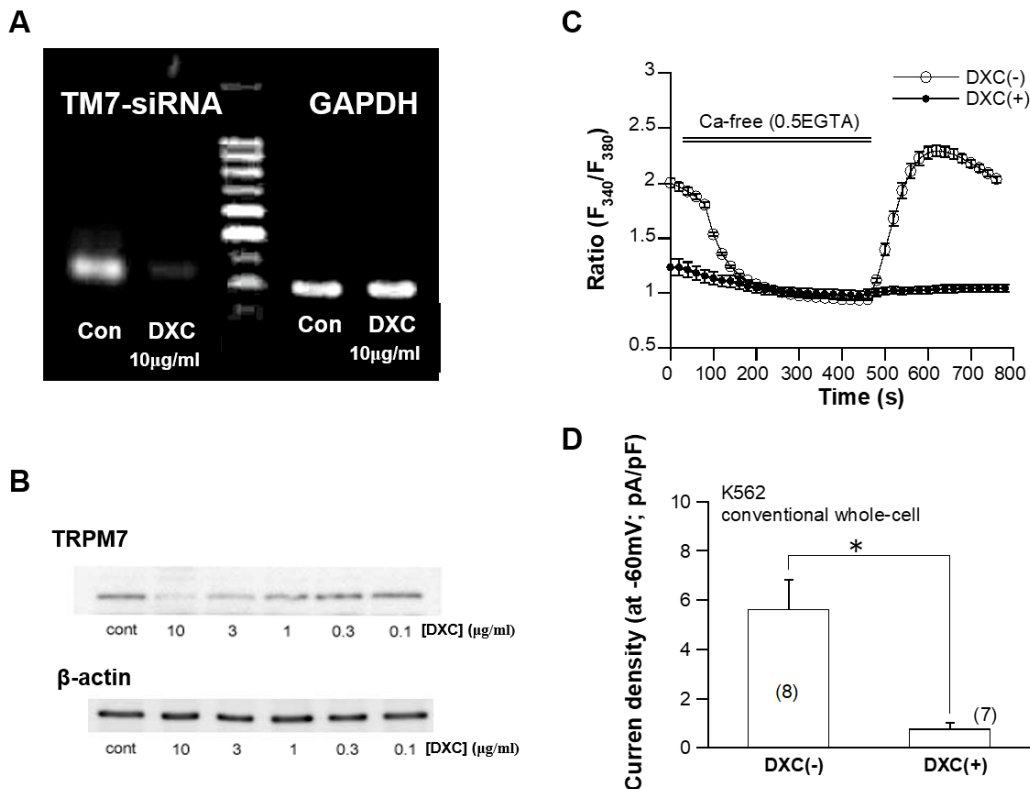


Fig.6 K562 cell growth is dependent on  $\text{Ca}^{2+}$  influx mediated by TRPM7 channel

A; Dependency of K562 cell growth on extracellular  $\text{Ca}^{2+}$  concentration evaluated at 72hrs after culture. Open and filled circles indicate K562 cells untreated [DXC(-)] or treated with 10 $\mu\text{M}$  doxycycline [DXC(+)], respectively. B; time courses of K562 cell growth under various conditions, i.e. *DXC(-)* (no doxycycline and normal  $\text{Ca}^{2+}$  in RPMI medium), *DXC(-)0Ca<sup>2+</sup>* (no doxycycline and  $\text{Ca}^{2+}$  free in the medium), *DXC(+)* (10 $\mu\text{M}$  doxycycline and normal  $\text{Ca}^{2+}$  in the medium) and *DXC(+)*0 $\text{Ca}^{2+}$  (10 $\mu\text{M}$  doxycycline and  $\text{Ca}^{2+}$  free in the medium). In both types of experiments (A and B), K562 cells stably expressing *tet*-inducible TRPM7-siRNA (siTRPM7) were used. n=5 for each condition. \*: P<0.05 with two-way ANOVA with repeated-measures and Tukey's multiple comparison test. To avoid promiscuity, the results of statistical evaluation are shown only for selected pairs of groups.

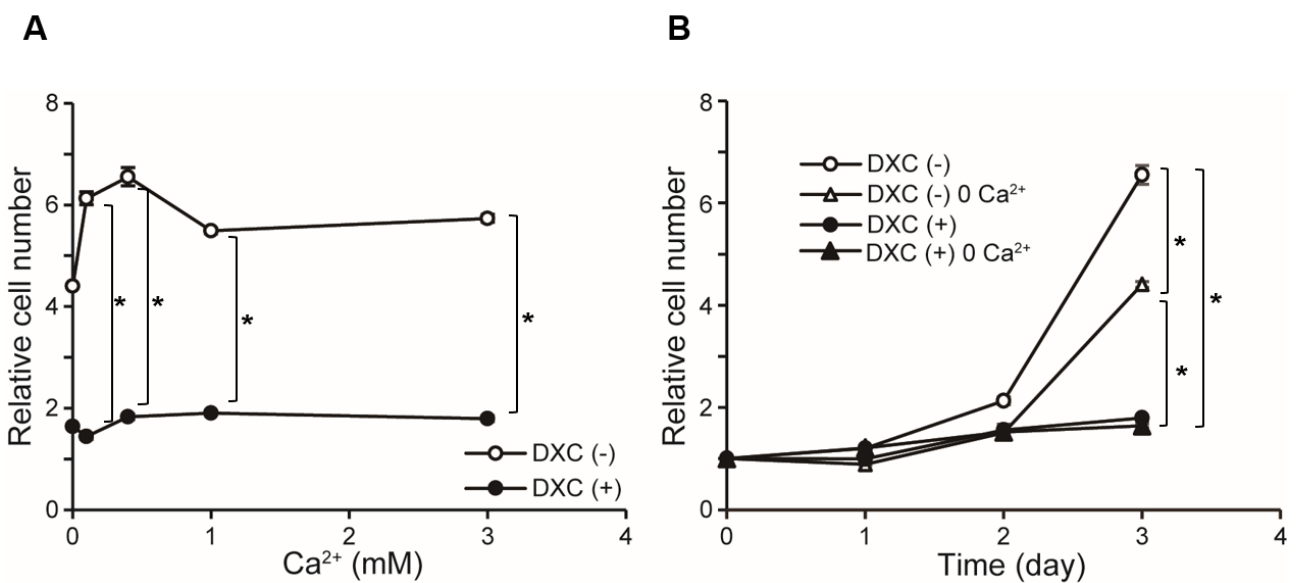


Fig.7 Erythroid differentiation of K562 cell by hemin is regulated by  $\text{Ca}^{2+}$  influx mediated by TRPM7. A; representative RT-PCR experiments showing hemin-induced  $\gamma$ -globin synthesis in K562 cells untreated (control) and treated with 10 $\mu\text{M}$  FTY720 (+FTY), 1mM EGTA (+EGTA) or 10 $\mu\text{M}$  doxycycline (+dxc). In all conditions, K562 cells stably expressing *tet*-inducible TRPM7-siRNA (siTRPM7) were used. The expression  $\gamma$ -globin mRNA was greatly decreased by these procedues, while that of GAPDH stayed almost constant. B, C; statistical evaluation of pooled data from experiments as shown in A: 10 $\mu\text{M}$  FTY720 and 1mM EGTA (B): siTRPM7 (C). D, E; effects of 10 $\mu\text{M}$  FTY720 (FTY), 1mM EGTA (EGTA) or 10 $\mu\text{M}$  doxycycline (+dxc) on haemoglobin synthesis at rest or 3days after hemin treatment in K562-cells stably expressing siTRPM7. n=5 for each condition. \*: P<0.05 with two-way ANOVA and Tukey's multiple comparison test. To avoid promiscuity, the results of statistical evaluation are shown only for selected pairs of groups.

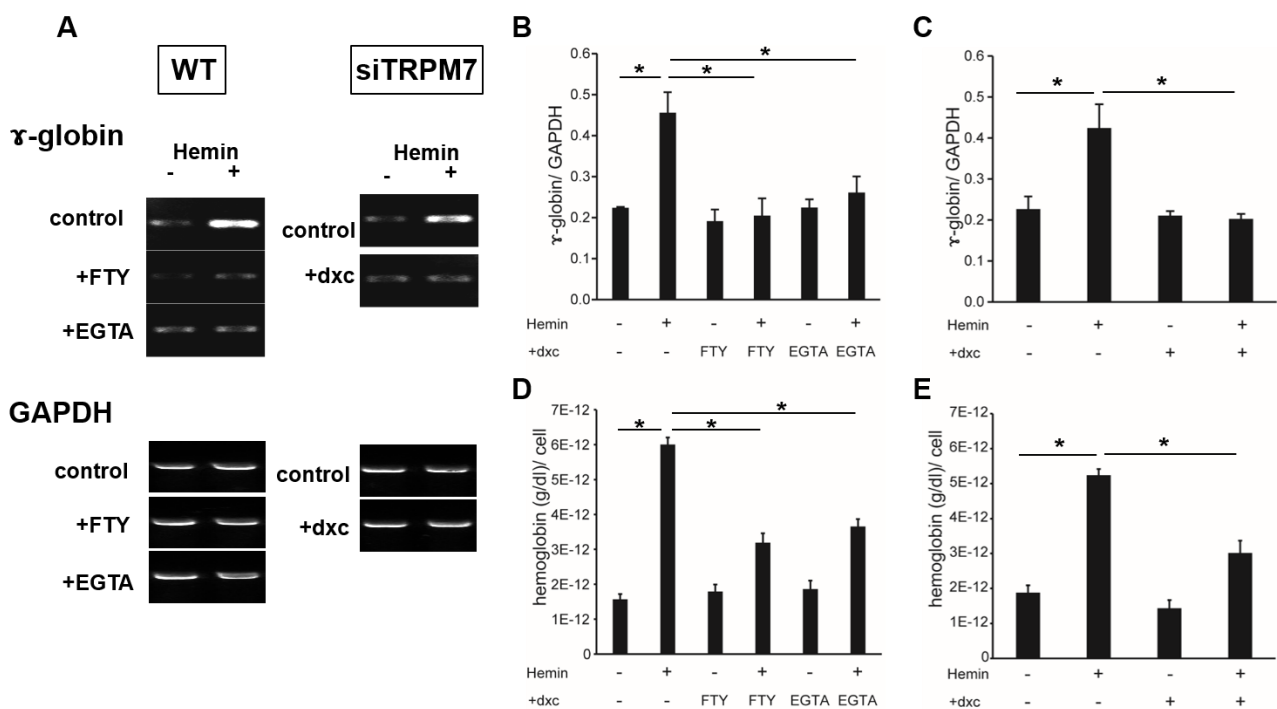
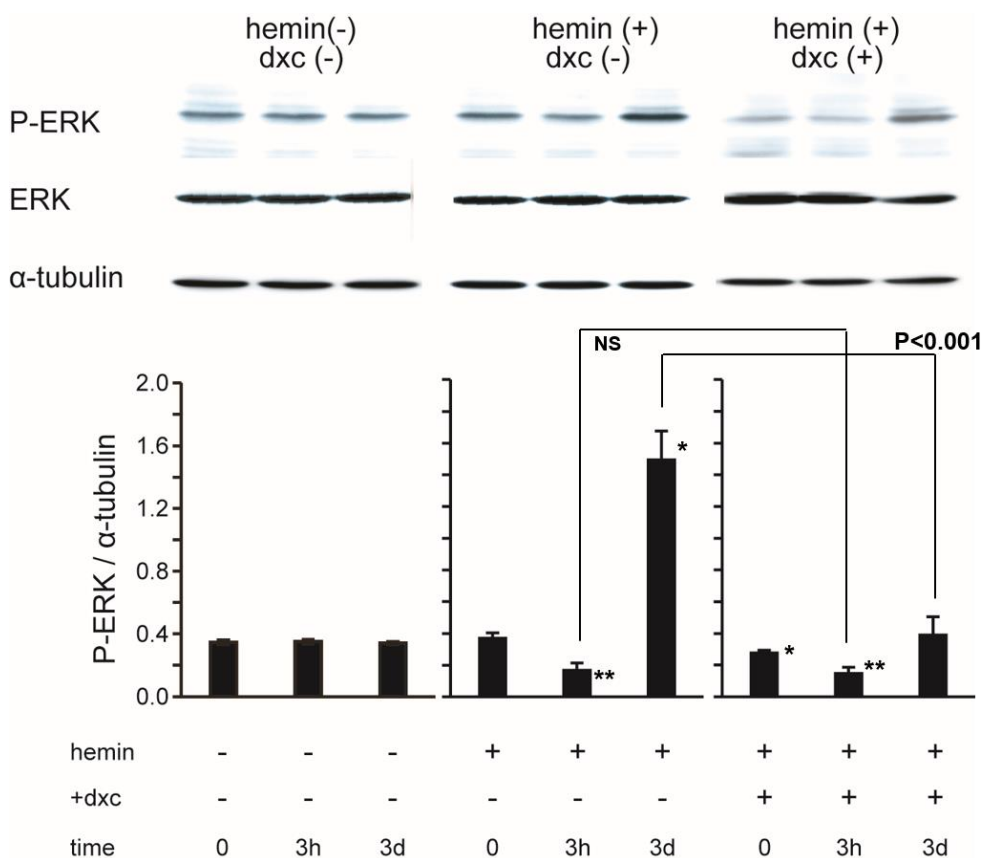


Fig.8 Time-dependent ERK phosphorylation under hemin stimulation without or with siTRPM7 treatment. The respective time courses of phosphorylated ERK, ERK and  $\alpha$ -tubulin protein expressions. Assessed by the immunoblotting technique from siTRPM7-expressing K562 cells untreated [hemin(-), dxc(-)] or treated with hemin [(hemin(+)], and/or doxycycline (+dxc) before (0hr) and 3hrs or 3days after the start of each experimental condition. Upper and lower panels indicate actual results and their relative expression levels (normalized to  $\alpha$ -tubulin protein expression which did not change during the course of experiments) averaged from 5 independent experiments, respectively. \*, and \*\* respectively indicate P values of <0.05 and <0.01 vs. the corresponding time controls (three leftmost columns) with Tukey's multiple comparison test. The results of Tukey's test for the columns paired by U-shaped lines are also shown.



## Supplementary Fig. 1

Hemin treatment does not affect TRPM7 activity.

TRPM7-mediated currents were measured by introducing ATP-free,  $Mg^{2+}$ -free internal solution (see the Methods) into non-treated or hemin ( $40\mu M$ , 3days)-treated K562 cells at a holding potential of  $-50mV$ . Data are expressed as the averaged current density (pA/pF) at  $-50mV$  after normalizing to the cell capacitance. The numbers in parentheses indicate those of independent measurements.

There is no statistically significant difference between non-treated and hemin-treated K562 cells with unpaired student t-test.

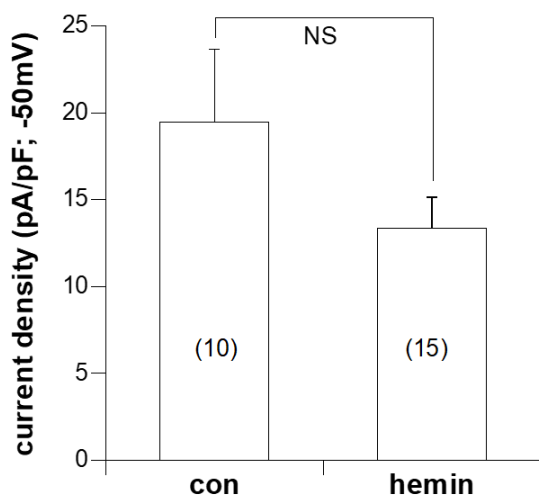
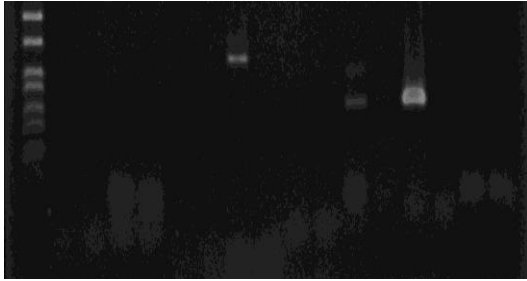


**Figure 1**

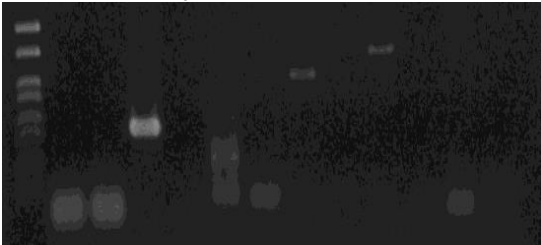
**A**

*TRPM family*



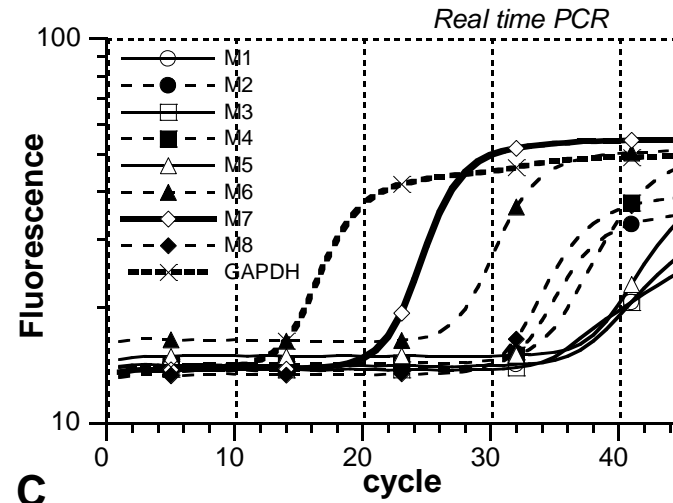
RT + - + - + - + - + - + -  
M1 M2 M3 M4 M5 M6 M7 M8

*TRPV family*

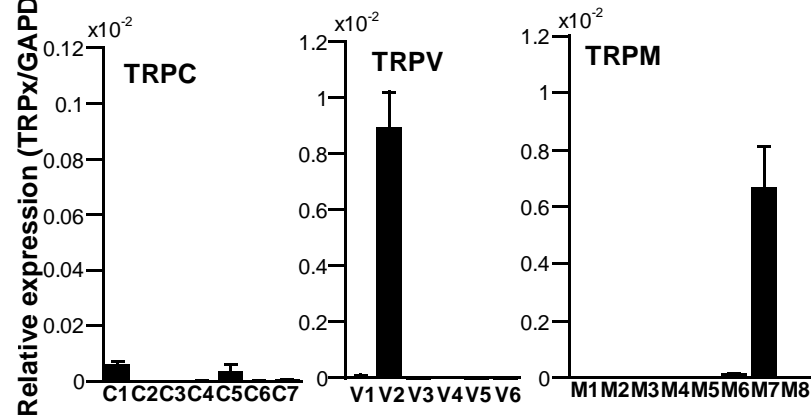


RT + - + - + - + - + - + -  
V1 V2 V3 V4 V5 V6

**B**

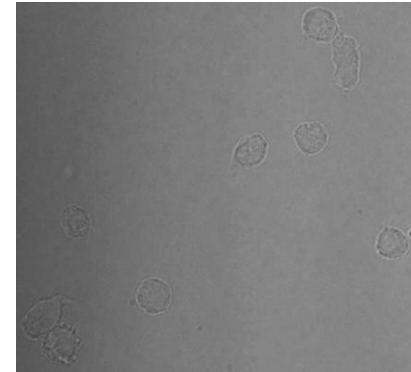


**C**



**D**

DIC



fluorescence

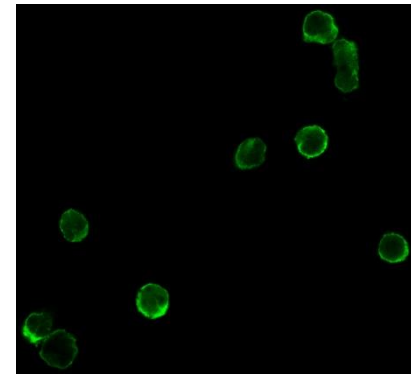
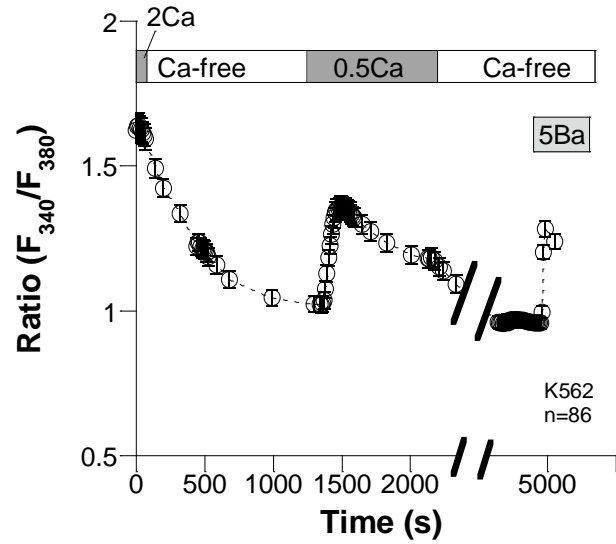
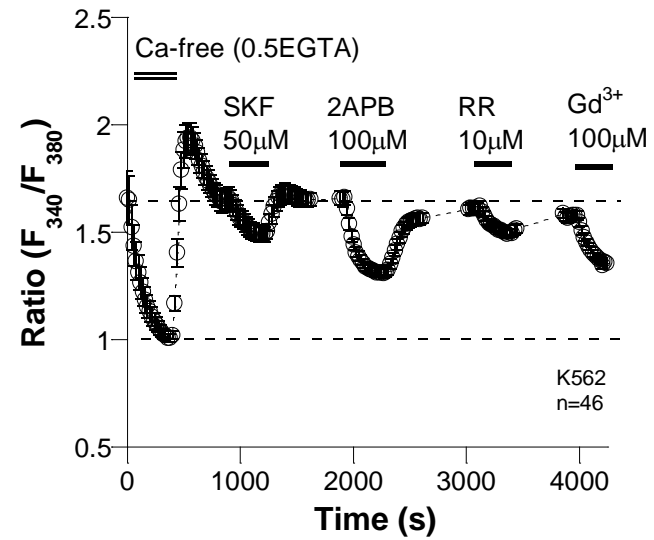


**Figure 2**

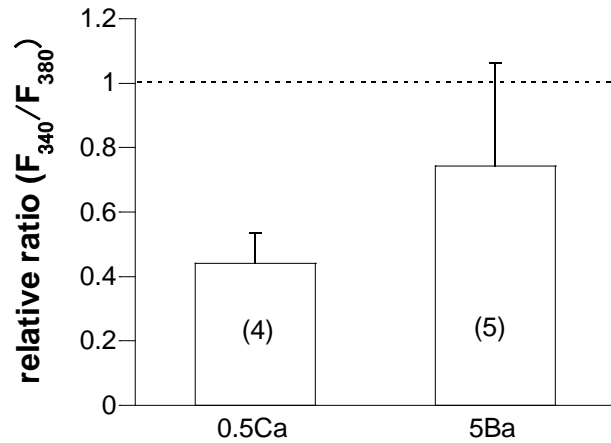
**A**



**B**



**C**



**D**

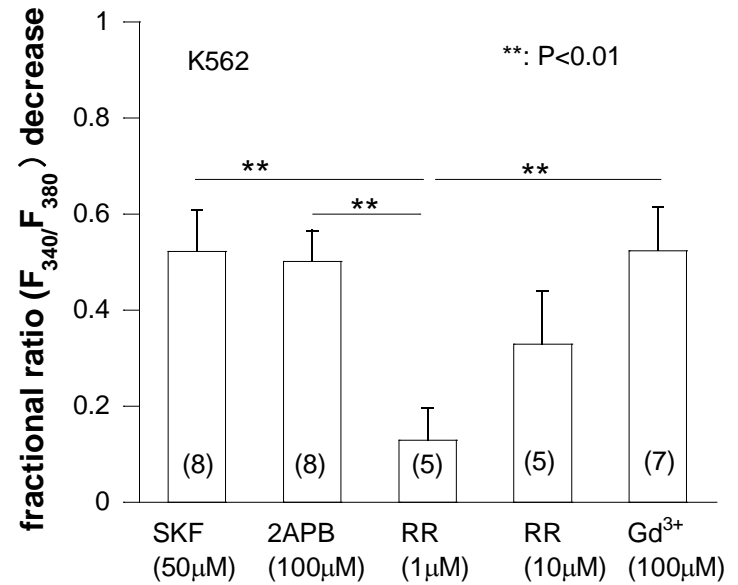
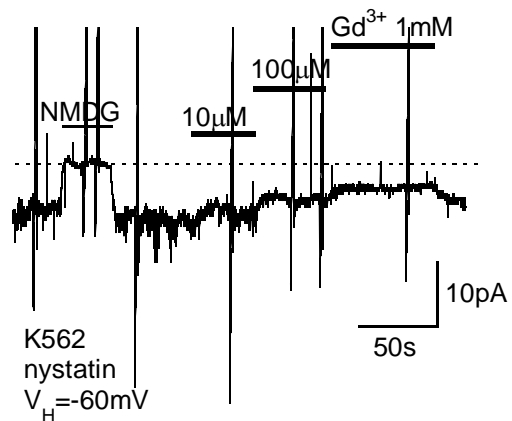


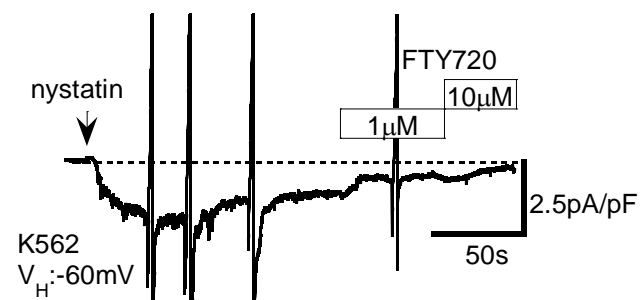


Figure 4

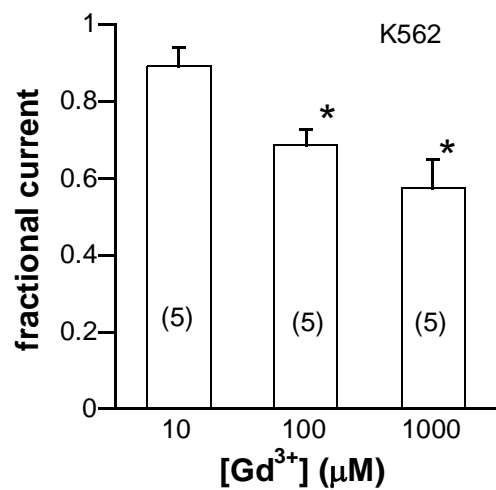
A



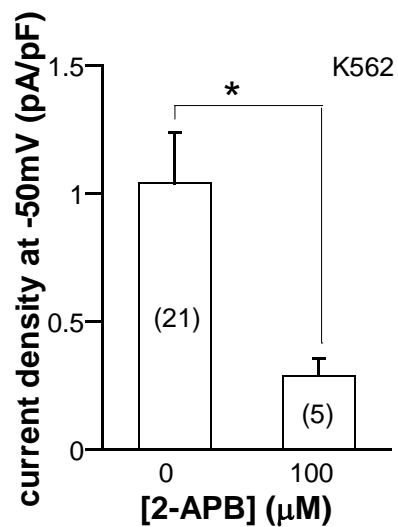
B



C



D



E

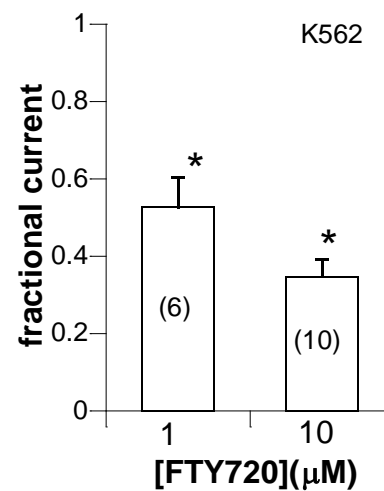
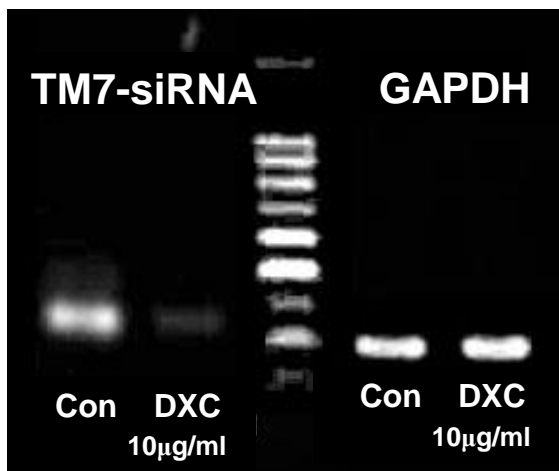
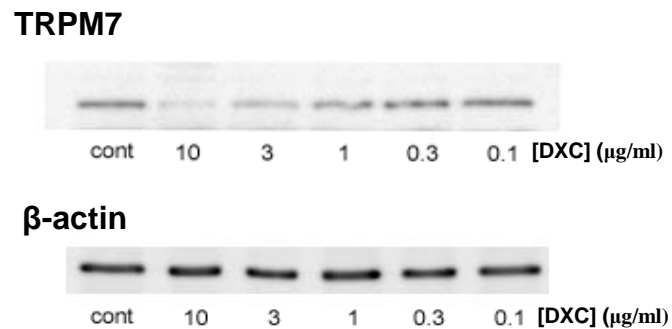


Figure 5

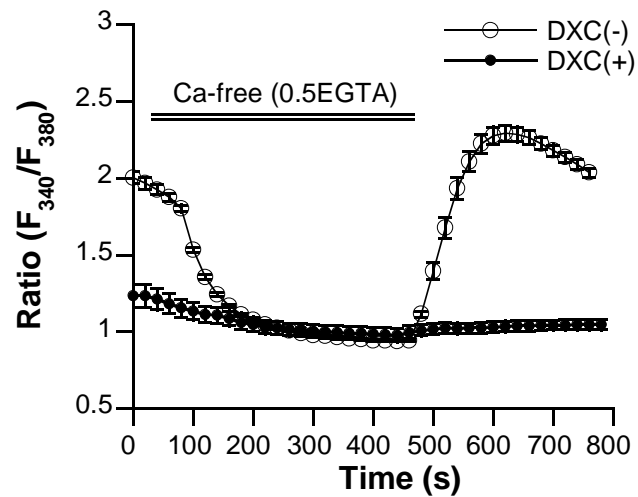
A



B



C



D

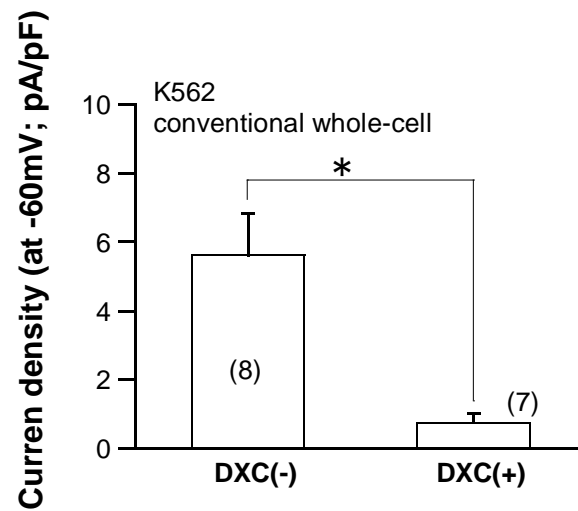
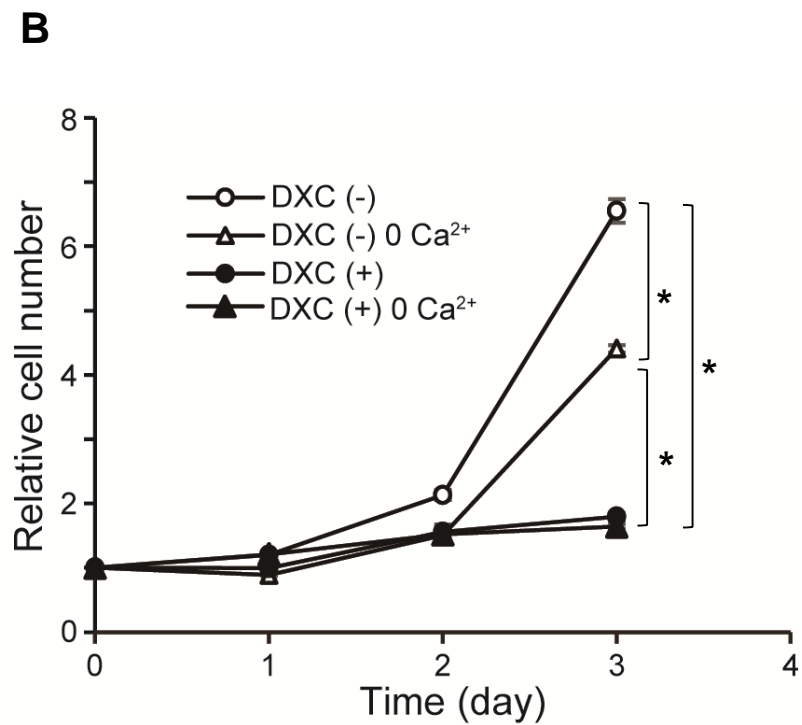
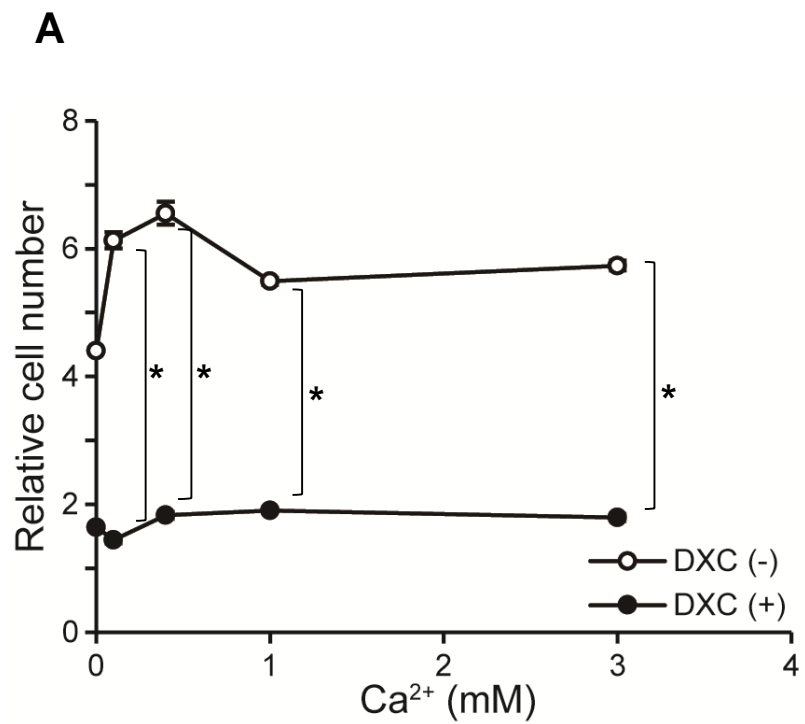
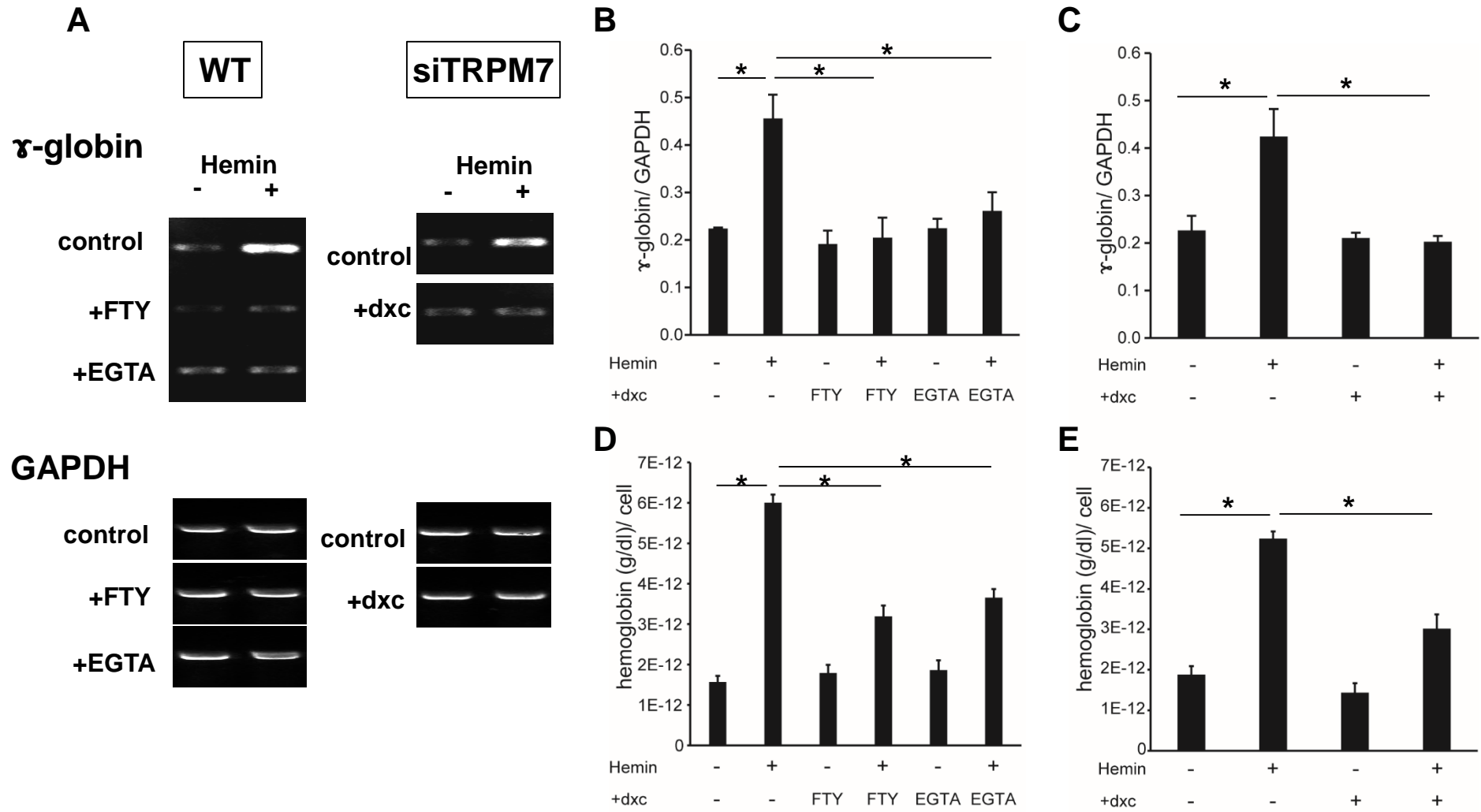


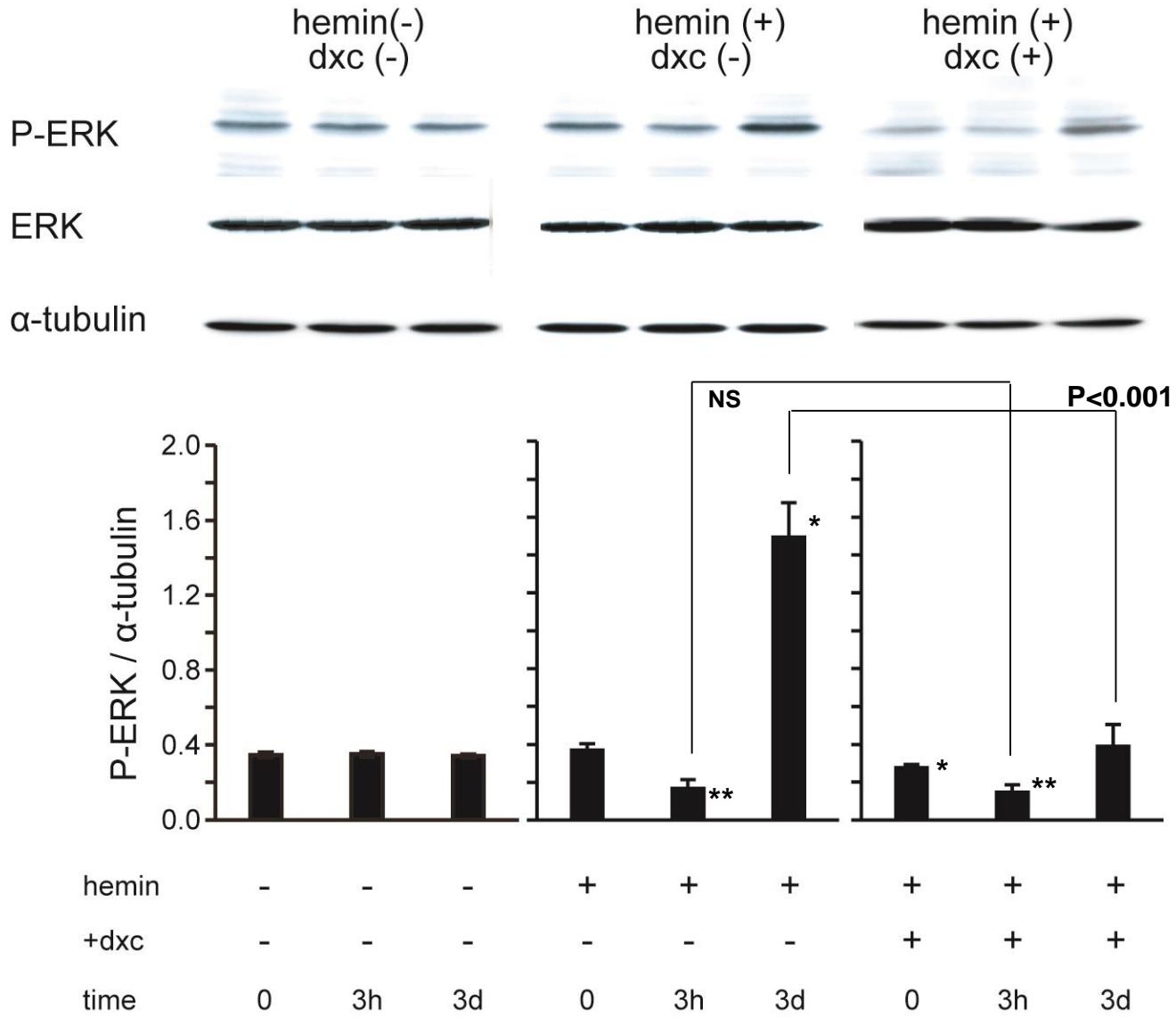
Figure 6



**Figure 7**



**Figure 8**



# Supplementary Figure 1

